Review

Functional Morphology of the Cardiac Jelly in the Tubular Heart of Vertebrate Embryos

Jörg Männer [1,*] and Talat Mesud Yelbuz [2]

[1] Group Cardio-Embryology, Institute of Anatomy and Embryology UMG, Georg-August-University Goettingen, D-37075 Goettingen, Germany; jmaenne@gwdg.de

[2] Department of Cardiac Sciences, King Abdulaziz Cardiac Center, Section of Pediatric Cardiology, King Abdulaziz Medical City, Ministry of National Guard Health Affairs; Riyadh, Kingdom of Saudi Arabia; yelbuzta@ngha.med.sa

* Correspondence: jmaenne@gwdg.de; Tel.: +49-551-39-7032

Abstract: The early embryonic heart is a multi-layered tube consisting of (1) an outer myocardial tube; (2) an inner endocardial tube; and (3) an extracellular matrix layer interposed between myocardium and endocardium, called "cardiac jelly" (CJ). During the past decades, research on CJ has mainly focused on its molecular and cell biological aspects. This review focuses on the morphological and biomechanical aspects of CJ. Special attention is given to (1) the spatial distribution and fiber architecture of CJ; (2) the morphological dynamics of CJ during the cardiac cycle; and (3) the removal/remodeling of CJ during advanced heart looping stages, which leads to the formation of ventricular trabeculations and endocardial cushions. CJ acts as a hydraulic skeleton displaying striking structural and functional similarities with the mesoglea of jellyfish. CJ not only represents a filler substance, facilitating end-systolic occlusion of the embryonic heart lumen. Its elastic components antagonize the systolic deformations of the heart wall and thereby power the refilling phase of the ventricular tube. Non-uniform spatial distribution of CJ generates non-circular cross sections of the opened endocardial tube (initially elliptic, later deltoid), which seem to be advantageous for valveless pumping. Endocardial cushions arise from non-removed remnants of the original CJ.

Keywords: Embryonic heart tube; extracellular matrix; cardiac jelly; hydraulic skeleton; heart skeleton; valveless pumping; blood flow; non-circular cross sections; ballooning; trabeculation

1. Introduction

The heart is the first organ to form and function in vertebrate embryos. During the initial phase of its pumping activity, the vertebrate heart has the design of a tubular conduit that generates unidirectional blood flow by a valveless pumping mechanism [1]. The wall of this tubular heart has a relatively simple architecture. It consists of only two different epithelial layers, from which one forms the outer envelope and the other forms the inner lining of the tube. The outer envelope of the heart tube, which is in contact with the pericardial fluid, is formed by a two-layered epithelium of embryonic cardiomyocytes, nowadays called the "primary myocardium" [2]. The inner lining of the heart tube, which is in contact with the blood, is formed by a single-layered endothelium called the primitive or "primary endocardium". The myo- and endocardial layers of the embryonic heart tube are not in direct contact with each other. Instead, a wide, cell-free space is found between them (Fig. 1).
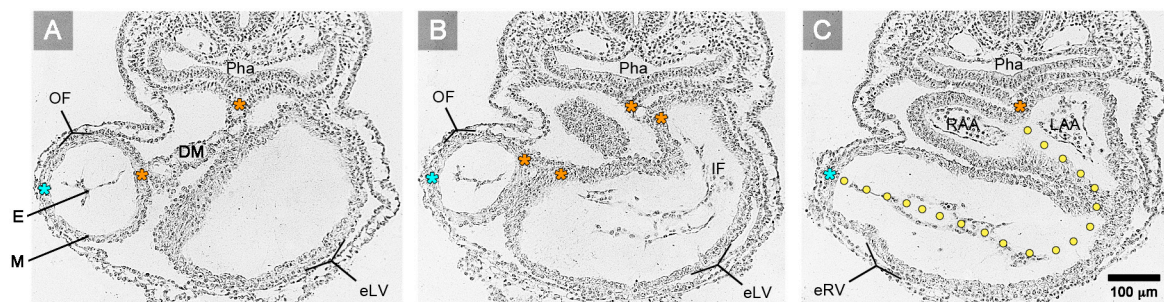

Figure 1. These transverse histological sections of a human embryo with 10 pairs of somites (Carnegie stage 10) show the inner architecture of an S-shaped heart tube as seen in routine histological preparations. The heart was fixed in a systolic state so that its lumen is partially obliterated. (**A**) Section at the level of the proximal outflow (=OF) of the ventricular tube. (**B**) Section of at the level of the inflow (=IF) of the ventricular tube. (**C**) Section at the level of the developing right and left atrial appendages (= RAA, LAA). Note that the myocardium (=M) and endocardium (=E) are separated by an "empty" space, called the myoendocardial space. Note also: (1) the difference in thickness of the myoendocardial space between the developing atria and ventricles; and (2) the paired character of the myoendocardial space, which reflects the origin of the heart from bilaterally paired heart fields. The dorsal mesocardium (=DM, and indicated by orange asterisks) and the obliterated endocardial tube can be used as anatomical landmarks for the original midsagittal fusion plane of the left- and right-sided heart fields (marked by the dotted line in section C). Light blue asterisks mark the original ventral midline of the heart tube. Further abbreviations: eLV = embryonic left ventricle; eRV = embryonic right ventricle; Pha = pharynx / foregut.

In the tradition of the Department of Embryology of the Carnegie Institution, this space was named the "myoendocardial space" [3-7]. During the 19th and early 20th century, the structure and material properties of the substance filling the myoendocardial space were deduced only from light microscopical observations on routine histological sections (Fig. 1), which showed either an "empty" space or a space filled with traces of "filamentous" material. Based on such morphological data, the content of the myoendocardial space was interpreted either as serous fluid [8,9] or as a cell-free, gelatinous material [10-12]. Based on *in vivo* observations on

75   chick embryonic hearts, Carl L. Davis was able to confirm the gelatinous character
76   of the transparent material filling the myoendocardial space and named it the
77   "cardiac jelly" [13]. His work, which has been published in the form of a meeting
78   abstract in 1924, may be regarded as an early landmark in research on the
79   extracellular matrix (ECM) of the early embryonic heart, since the term "cardiac
80   jelly" (CJ) found its way into the "Terminologia Embryologica" produced by the
81   "Federative International Committee on Anatomical Terminology" [14]. Today, the
82   term "cardiac jelly" (CJ) is frequently used synonymous for the myoendocardial
83   space of the early embryonic heart tube.

84   Classical embryology did not pay much attention to the CJ and other forms of
85   embryonic ECM [15]. Therefore, its structure, composition and functions remained
86   obscure for a long time following the confirmation of its gelatinous character. The
87   first study on the function of CJ was published in 1948 [16]. In this pioneering work,
88   Alexander Barry related the presence of a thick myoendocardial layer of viscoelastic
89   CJ to biophysical functions, namely the mechanical support of valveless pumping.
90   He used geometric calculations to show that the presence of a relatively thick layer
91   of CJ is required for complete end-systolic occlusion of the lumen of vertebrate
92   embryonic heart tubes (Fig. 2). This was thought to improve the efficiency of the
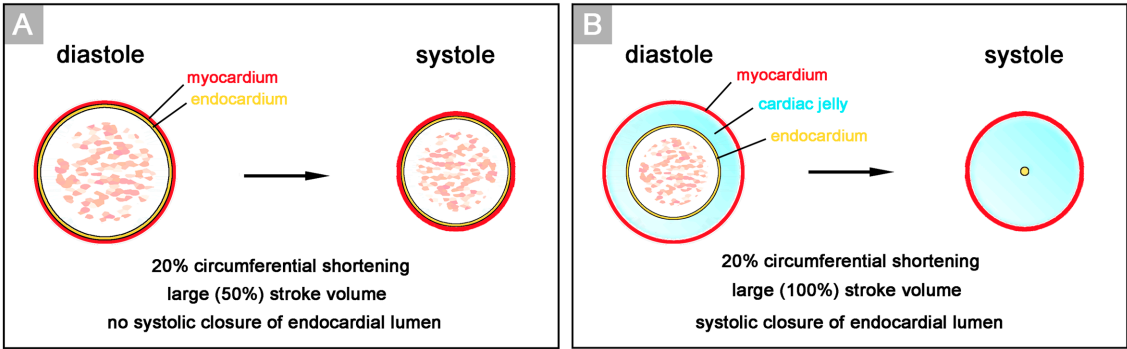93   pump action of the valveless heart tube by preventing backflow of blood.
94

95   **Figure 2.** These schematic drawings illustrate Barry's geometrical analyses on cross sections of
96   hypothetical heart tubes of large diameter. (**A**) In a hypothetical heart tube without CJ, physiological
97   shortening of the contracting myocardium (20%) produces a large change (50%) in cross sectional
98   area of the lumen (= stroke volume), but does not close the lumen. (**B**) In a hypothetical heart tube
99   with CJ, physiological shortening of the contracting myocardium will produce a large change (100%)
100   in stroke volume as well as complete closure of the endocardial lumen, if the thickness of the CJ layer
101   is about 45% of the radius of the diastolic lumen. Note that the spatial distribution of CJ in the
102   hypothetical heart tube does not correspond to the non-uniform distribution of CJ (bilaterally paired
103   character) found in real embryonic heart tubes (see Fig. 1A).

104   Barry, furthermore, has speculated that the diastolic reopening of the lumen of the
105   embryonic heart tube is powered by passive energy stored in the elastic
106   deformation of the CJ during systole. This mechanism was said to explain the
107   diastolic sucking action of heart tubes, which he observed in experiments on living
108   chick embryos. Barry's ideas about the role of the CJ in the normal pumping
109   function of valveless embryonic heart tubes are supported by the phenotype of

110 CJ-deficient mouse embryos, which show signs of severe heart insufficiency during
111 the initial phase of embryonic heart action [17].
112   In the years following Barry's pioneering work, there was little interest in
113 uncovering of further biophysical functions of the CJ. The research has mainly
114 focused on the biochemical composition of the CJ, its dynamic changes during
115 development, and the cell biological effects of CJ components [reviewed by 18].
116 Research on organ-scale biophysical functions of the CJ and its structural
117 background had a short revival in the late 1970ies and early 1980ies. Manasek and
118 coworkers have shown that the hydration of the CJ generates a turgor pressure that,
119 together with a network of delicate CJ fibers, stabilizes the shape of the outer
120 myocardial tube in a manner comparable to an inflated balloon [19,20]. These data
121 indicate that the CJ behaves as a "hydraulic skeleton" and, therefore, may be
122 regarded as the first skeleton of the vertebrate heart [for reviews about hydraulic
123 skeletons see 21-23]. Manasek and coworkers have, furthermore, speculated that
124 hydraulic expansion of the CJ, together with unisotropic arrangement of fibrils
125 within the myocardial envelope, may drive the deformation of the initially straight
126 embryonic heart tube into a helically coiled heart loop [19,20,24]. The idea of
127 CJ-driven heart looping, however, was disproved by the observation that
128 experimental removal of CJ at pre-looping stages did not prevent cardiac looping in
129 mouse and chick embryos [25,26].
130   We should note here that the phenotype of a jelly-like ECM is not specific for
131 the early embryonic heart. It merely represents the generalized phenotype of early
132 embryonic ECMs [11,27]. Thus, CJ is only a local variant of a group of embryonic
133 ECMs that may be termed "embryonic jellies". The high hydration of embryonic
134 jellies generate turgor pressures that, together with extracellular fiber systems and
135 epithelial walls, contribute to mechanical stabilization of the shape of the early
136 embryo and some of its organs [11,27]. Therefore, besides several other currently
137 known functions, embryonic jellies act as hydraulic skeletons.
138   The short phase of revived interest in the organ-scale biophysics of CJ was
139 followed by a relatively long phase of remarkable progress in our understanding of
140 the molecular and cell biological aspects of the CJ. The continuous progress in
141 knowledge about the functional significance of the early cardiac ECM was
142 documented in several excellent review articles, which appeared over the last 20
143 years [28-31]. While reading these papers, we have noted, to our surprise, that the
144 contributions of the CJ to the pumping mechanics of the embryonic heart tube were
145 either completely ignored [28,30] or were reduced to the cryptic statement that CJ
146 helps "regulation of blood flow" [29,31]. Comments on the significance of the CJ for
147 the mechanical pump action of the early embryonic heart tube are also missed in
148 contemporary monographs and textbooks on cardiac development [32,33]. Proper
149 pumping function of the tubular embryonic heart is crucial for survival of higher
150 vertebrate embryos as well as for correct morphogenesis of their hearts [34,35].
151 Thus, a deep understanding of the morphogenesis of congenital heart defects needs
152 understanding of the ontogeny of cardiac pumping function. This, in turn, will

153 remain fragmentary without knowledge about the organ-scale mechanics of the CJ
154 and its structural base.
155   This review article is intended to close the above-mentioned gap of knowledge
156 found in contemporary reviews about the ECM of the early embryonic heart. Our
157 paper, therefore, focuses exclusively on the currently neglected morphological and
158 biomechanical aspects of CJ. We hope that this article will contribute to a better
159 understanding of the morphogenesis and pumping function of the early embryonic
160 heart of vertebrates.

2. Definition of Terms and Chronology of CJ Development

162   Davis introduced the term "cardiac jelly" (CJ) for characterization of the
163 cell-free, gelatinous substance filling the myoendocardial space of the embryonic
164 heart tube [13]. In this review article we define CJ in this strict sense. According to
165 this definition, the ECM of the early embryonic heart will be called CJ if it fulfills
166 two requirements: (1) the ECM has to occupy an anatomically well-demarcated
167 myoendocardial space that is bordered by the basal laminae of the primary
168 myocardium and endocardium; and (2) the ECM has to be free of cells.
169   These two conditions are present together only during a relatively narrow
170 time span of early cardiogenesis. This period starts with the first appearance of an
171 anatomically well-demarcated myoendocardial space and ends in a region-specific
172 manner either with the invasion of endocardium-derived mesenchymal cells into
173 the CJ (atrio-ventricular canal and outflow portion of the heart tube) or with the
174 formation of a trabeculated myocardial wall (ventricular bend of the heart tube).
175   The timing of the first appearance of an anatomically well-demarcated
176 myoendocardial space depends on the structural development of the primary
177 myocardium and the formation of endocardium-lined tubes (Fig. 3). Both
178 components of the wall of the embryonic heart tube derive from bilaterally paired
179 areas of the visceral layer of the lateral plate mesoderm. These areas are called the
180 "pre-cardiac mesoderms" or the "heart fields". The pre-cardiac mesoderms harbor
181 two different progenitor cell populations. These are (1) myocardial progenitors
182 (pre-myocardium), which form the coelomic epithelium of the heart fields; and (2)
183 endocardial progenitors (pre-endocardium), which are found in close spatial
184 association with the endoderm. The pre-cardiac mesoderms, furthermore, harbor a
185 gelatinous ECM, which connects the pre-myocardium and pre-endocardium with
186 each other, and with the endoderm (Fig. 3). This ECM layer, which likely becomes
187 incorporated into the CJ of the prospective heart tube, was called CJ in a few
188 previous publications [e.g. 36,37]. However, we prefer usage of the term
189 "pre-cardiac ECM". This is mainly for the following reason. The pre-myocardium
190 does not possess a continuous basal border to the pre-cardiac ECM, and the
191 pre-endocardium is a population of scattered mesenchymal cells embedded in the
192 pre-cardiac ECM (Fig. 3). Consequently, the pre-cardiac mesoderms initially do not
193 possess well-formed anatomic borders that demarcate a myoendocardial space
194 devoid of cells. The pre-cardiac ECM has the character of an intercellular substance
195 that glues together the cellular elements of the pre-cardiac mesoderms and,

therefore, should not be regarded as a cell-free ECM compartment. Appearance of an anatomically well-demarcated myoendocardial space depends on the differentiation of the pre-myocardium and pre-endocardium into the primary myocardium and endocardium-lined tubes, respectively (Fig. 3). During myocardial differentiation, the initially discontinuous basal layer of the pre-myocardium becomes transformed into a continuous cell sheet bordered by a basal lamina. As a consequence, the developing myocardium becomes an anatomically well-demarcated two-layered epithelium and the pre-cardiac ECM becomes split into two compartments; (1) a small compartment, which fills the intercellular spaces within the primary myocardium (intramyocardial ECM), and (2) a large, cell-free compartment, which fills the developing myoendocardial space (cardiac jelly).
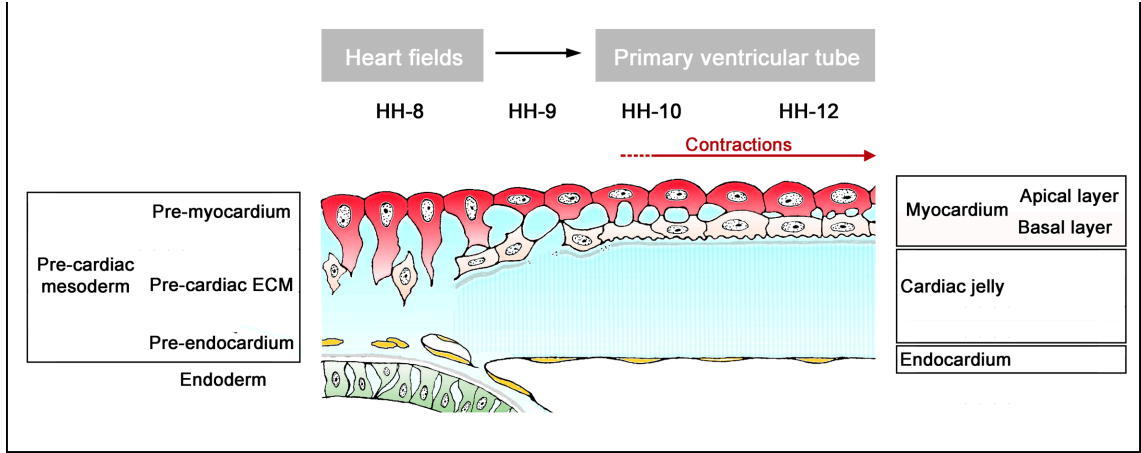

Figure 3. This schematic drawing illustrates the establishment of the primary wall architecture and initiation of myocardial contractions in the tubular hearts of higher vertebrate embryos as seen in chick embryos (based on data from Manasek [36] and Sakai et al., [38]). The components of the primary heart wall (primary myocardium, CJ, primary endocardium) derive from the pre-cardiac mesoderms/heart fields. The pre-cardiac mesoderms harbor: (1) myocardial progenitors (pre-myocardium), which form the coelomic epithelium of the heart fields; and (2) endocardial progenitors (pre-endocardium), which are found in close spatial association with the endoderm. The pre-cardiac mesoderms, furthermore, harbor a gelatinous ECM (pre-cardiac ECM), which connects the pre-myocardium and pre-endocardium with each other, and with the endoderm. The pre-cardiac mesoderms do not possess an anatomically well-demarcated myoendocardial space. Its ECM acts as an intercellular substance that glues together the cellular elements of the pre-cardiac mesoderms. Appearance of an anatomically well-demarcated myoendocardial space depends on the differentiation of the primary myocardium and the formation of endocardium-lined tubes. During myocardial differentiation, the originally discontinuous basal layer of the pre-myocardium becomes transformed into a continuous cell sheet bordered by a basal lamina. As a consequence, the developing myocardium becomes an anatomically well-demarcated two-layered epithelium and the pre-cardiac ECM becomes split into: (1) a small compartment, which fills the intercellular spaces within the primary myocardium (intramyocardial ECM), and (2) a large, cell-free compartment, which fills the developing myoendocardial space (CJ).

It is well known that the chronology of the morphogenetic processes contributing to early cardiogenesis differs markedly across vertebrate species [39,40]. It is, therefore, no wonder that the relation between the timing of the first

231 appearance of an anatomically well-demarcated myoendocardial space and the
232 timing of the emergence of the embryonic heart shows species-specific differences.
233 The initially straight heart tube of vertebrate embryos is a single median structure
234 that arises from the union of materials from bilaterally paired heart fields in front of
235 the developing foregut [41]. In some mammalian species, such as rabbits [42,43],
236 rats [44,45], cats [46], and tree screws [40], myocardial differentiation and
237 establishment of the primary heart wall architecture precedes the union of the
238 paired heart fields. In these species, a bilateral pair of endocardial tubes,
239 surrounded by CJ and a contracting myocardial mantle, is formed within the two
240 heart fields shortly before the latter start their union along the ventral midline of the
241 foregut to form the single median heart tube. In this situation, the median heart
242 tube seems to arise from the union of a pair of actively pulsating blood vessels,
243 which have been named "lateral hearts" (42-45). In other vertebrate species, such as
244 chicks [47,48] or the frog *Xenopus laevis* [49], however, myocardial differentiation
245 and establishment of the primary heart wall architecture occurs in the median heart
246 tube, that means after the heart fields have started their union. In these species, the
247 first contractions of the developing myocardium were recorded in the median heart
248 tube [38,50]. Thus, comparative embryology shows that the establishment of an
249 anatomically well-demarcated myoendocardial space, filled with CJ, obviously,
250 does not depend on the establishment of a single median heart tube, but rather
251 correlates with the structural and functional differentiation of the myocardium and
252 endocardium.
253   Union of the bilaterally paired heart fields/lateral hearts starts at the level of the
254 prospective apical trabeculated regions of the ventricles from where it progresses
255 toward the venous as well as arterial poles of the single median heart tube, thereby
256 adding the primordia of further building elements (atrio-ventricular canal, atriums,
257 sinus venosus, ventricular outflow) to the developing heart [41]. During the initial
258 steps of heart field union, no significant differences in the wall architecture are
259 found along the length of the forming median heart tube. At advanced stages of
260 establishment of the median heart tube, however, regional differences in thickness
261 of the CJ layer become apparent along its length, which facilitate distinction of two
262 main building units. These units are (1) a sac-shaped venous chamber, which has
263 only a thin layer of CJ, and (2) a tube-shaped arterial conduit, which has a thick
264 layer of CJ (Figs. 1C and 4A). The sac-shaped unit gives rise to the prospective atria
265 and, therefore, may be called the "primary atrium", while the tube-shaped conduit
266 gives rise to the prospective ventricles and, therefore, may be called the "primary
267 ventricular tube" [6,9,51,52]. Cardiac looping morphogenesis transforms the
268 initially straight ventricular tube into a looped ventricular tube consisting of three
269 portions: (1) inflow, (2) ventricular bend, and (3) outflow. Due to the presence of a
270 thick CJ layer, the inflow and outflow portions possess relatively well-defined
271 anatomical borders to the primary atrium and aortic sac, respectively. They do not
272 possess, however, well-defined anatomical borders to the ventricular bend.
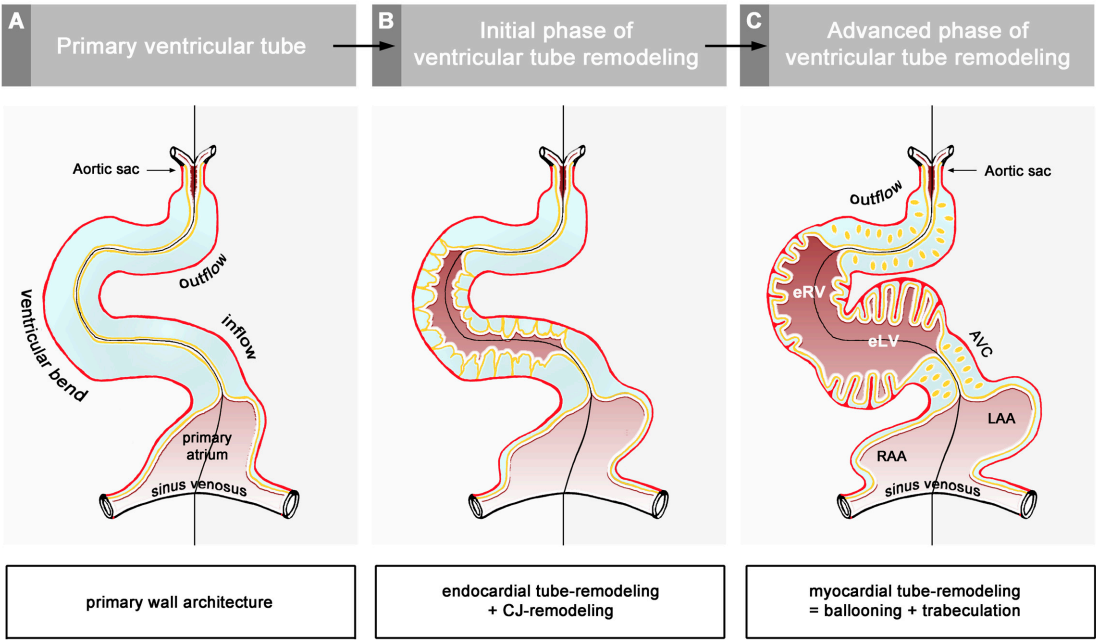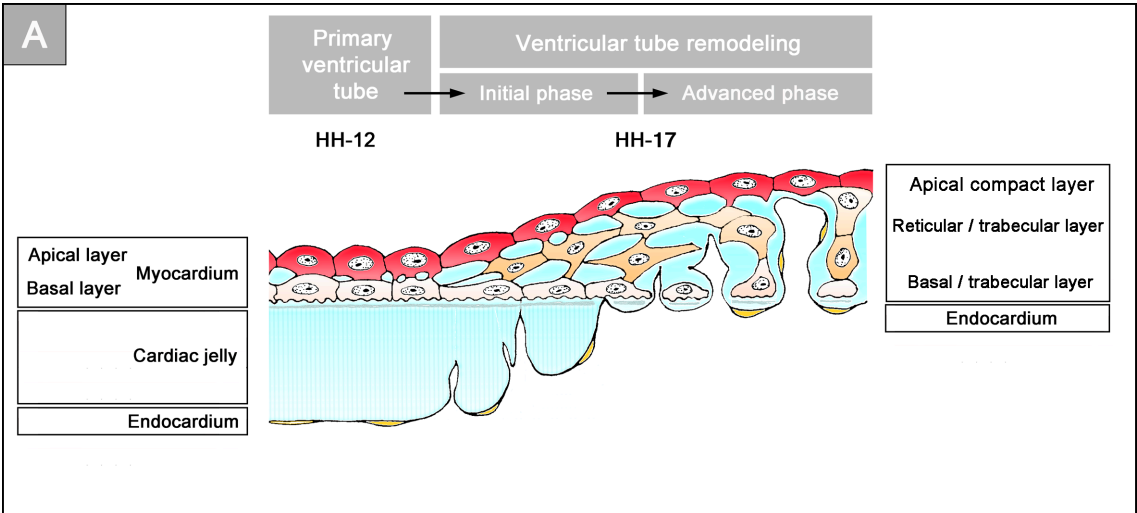273

Figure 4. These schematic drawings illustrate three subsequent phases in development of the wall architecture of the median embryonic heart tube of higher vertebrates. (**A**) **Primary wall architecture** (red = primary myocardium; light blue = CJ; yellow = primary endocardium). Local variations in thickness of the CJ layer facilitate distinction of two main building units: (1) a sac-shaped venous chamber, which has only a thin CJ layer and represents the primary atrium; and (2) a tube-shaped arterial conduit, which has a thick CJ layer and represents the primary ventricular tube. Presence of a thick CJ layer facilitates complete end-systolic occlusion of the endocardial lumen of all portions of the primary ventricular tube. Paired pattern of CJ accumulation reflects the origin of the ventricular tube from bilaterally paired heart fields. (**B**) The **initial phase of ventricular tube remodeling** is characterized by remodeling of the endocardial tube and CJ along the convexity of the ventricular bend. Endocardial sprouts/protrusions invade the CJ and grow toward the primary myocardium. As a consequence, CJ disappears along the convexity of the ventricular bend. (**C**) The **advanced phase of ventricular tube remodeling** is characterized mainly by remodeling of the myocardium along the convexity of the ventricular bend and by remodeling of the CJ in the ventricular inflow (atrio-ventricular canal) and outflow portions. Endocardial protrusions invade the myocardial wall, which starts centrifugal growth (ballooning and trabeculation). The CJ in the atrio-ventricular canal (AVC) and outflow does not disappear but becomes remodeled into endocardial cushions/ridges due to invasion of endocardium-derived mesenchymal cells. Abbreviations: eLV = embryonic left ventricle; eRV = embryonic right ventricle; LAA = anlage of left atrial appendage; RAA = anlage of right atrial appendage.

The thick layer of CJ, characterizing the primary wall architecture of the ventricular tube, facilitates complete end-systolic occlusion of the endocardial lumen of all portions of the ventricular tube (inflow, ventricular bend, outflow) and, thereby, supports the initial pumping action of the valveless embryonic heart [16]. Subsequent to the establishment of a hemodynamically effective pulsatile blood flow, however, a remodeling process starts within the ventricular tube that transforms its primary wall architecture and finally leads to the disappearance of a cell-free, gelatinous ECM (CJ). This remodeling process proceeds from the inside to the outside of the ventricular tube and can be subdivided into two phases, which we call the "initial" and "advanced phase of ventricular tube remodeling" (Figs. 4B

304 and C). The initial phase of ventricular tube remodeling is characterized mainly by
305 regionally confined remodeling of the endocardial tube and its surrounding CJ.
306 Except for internal structural changes (formation of a reticular layer), the
307 myocardial tube does not significantly change the primary smooth-walled
308 phenotype of its apical and basal surfaces (4B and 5A,B). The architectural changes
309 of the endocardial tube and CJ are regionally confined to the convexity of the
310 ventricular bend. Here, the endocardial tube forms multiple sprout- or
311 pouch-shaped outgrowths that invade the CJ and grow toward the basal surface of
312 the primary myocardium. As a consequence, CJ disappears along the convexity of
313 the ventricular bend [6,53-55]. The advanced phase of ventricular tube remodeling
314 is characterized mainly (1) by remodeling of the myocardium along the convexity of
315 the ventricular bend and (2) by remodeling of the CJ in the inflow and outflow
316 portions of the ventricular tube (Figs. 4C and 5A,B). The above-mentioned
317 endocardial sprouts/pouches now invade the myocardial wall along the convexity
318 of the ventricular bend and establish a primitive blood supply to the developing
319 myocardium. The affected areas of the ventricular myocardial wall undergo an
320 aneurysm-like expansion, – nowadays called ventricular "ballooning" [56] -- , and
321 acquire a trabeculated wall architecture [6,54]. The ventricular bend, thereby, looses
322 its primary tubular shape and starts formation of externally visible ventricular
323 chambers. In contrast to the convexity of the ventricular bend, the inflow (AVC)
324 and outflow portions of the ventricular tube keep their primary tubular shape as
325 well as their primary thick myoendocardial spaces for a relatively long time. The CJ
326 of these regions, however, becomes invaded by endocardium-derived
327 mesenchymal cells and, thereby, looses its cell-free phenotype and changes its
328 biophysical properties (e.g. stiffness) [27,57,58]. The paired accumulations of
329 cellularized CJ are named endocardial cushions (in the AVC) or endocardial ridges
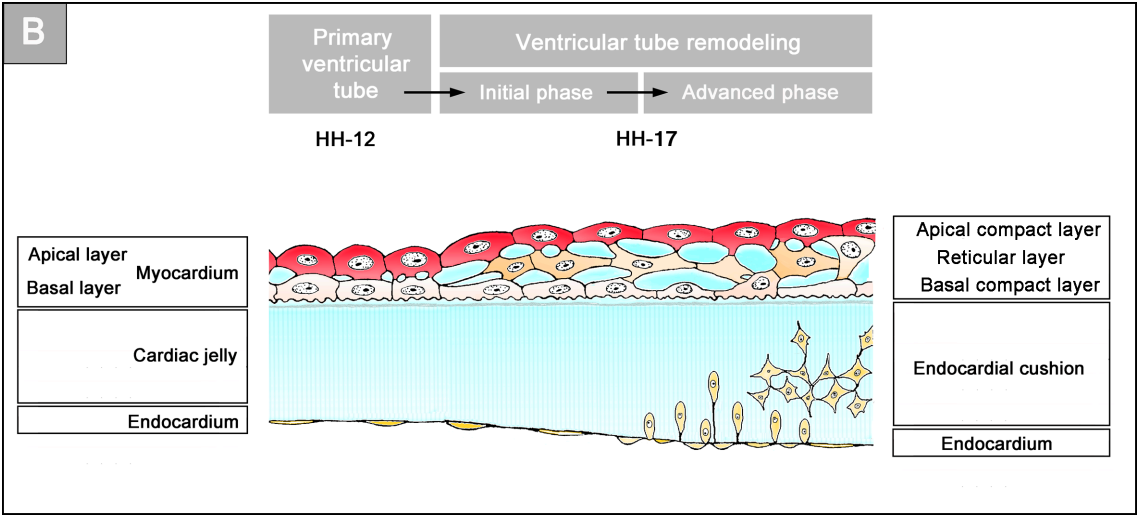330 (in the outflow).
331

Figure 5. These schematic drawings illustrate the region-specific remodeling of the primary ventricular tube of higher vertebrate embryos as seen in the chick (based on data from Manasek [53] and Icardo and Fernandez-Terán [54]). (**A**) **Remodeling along the outer curvature of the ventricular bend**. CJ disappears due to the outgrowth of multiple endocardial pouches from the endocardial tube (initial phase of remodeling). When the endocardial pouches reach the basal layer of the myocardium, they start invasion of the myocardial wall. Now, remodeling is no longer confined to the endocardium and CJ but, additionally, changes the wall architecture of the myocardial tube. The initially smooth myocardial wall becomes transformed into a trabeculated myocardial wall (advanced phase of remodeling). (**B**) **Remodeling in the inflow (AVC) and outflow portions of the ventricular tube**. CJ does not disappear but looses its cell-free phenotype and changes its biophysical properties due to the invasion of endocardium-derived mesenchymal cells. The paired accumulations of remodeled CJ are named endocardial cushions (in the AVC) or endocardial ridges (in the outflow).

Having presented an overview on the chronology of CJ morphogenesis, we will now describe the morphological dynamics of the CJ and its biomechanical implications during the above-mentioned three phases of early heart wall development.

3. Morphology and Function of the CJ in the Primary Ventricular Tube

In the preceding paragraphs we have seen that, in the so-called heart tube of vertebrate embryos, only the ventricular component has a tubular shape and a thick CJ layer while the atrial component is sac-shaped and has only a thin CJ layer. These differences in shape and wall architecture are associated with differences in the contraction behavior of the two components. While the wall of the primary atrium contracts in a more or less synchronous fashion, the wall of the primary ventricular tube contracts in the fashion of a traveling wave that starts at the ventricular inflow and travels along the tube toward the end of its outflow portion. At the present time, it is unclear whether these traveling waves reflect a peristaltic- or Liebau effect-driven pumping action of the primary ventricular tube [1]. With respect to the biomechanical function of the ventricular CJ, however, this fact does not seem to be a problem, since analyses on heart tube models have shown that both pumping mechanisms profit from the presence of a thick layer of CJ [16,59].

363   Based on geometrical analyses, Barry has shown that the thick layer of CJ acts as a
364   passive filler substance that facilitates complete end-systolic occlusion of the
365   ventricular endocardial tube at physiological rates of myocardial shortening [16].
366   His calculations were based on hypothetical heart tubes of simplified geometry in
367   which all three wall-layers had a perfect circular cross-section. This means that the
368   CJ-layer was of uniform thickness around the wall of the hypothetical heart tube
369   (Fig. 2B). Similar geometrical considerations were carried out by other researchers
370   to demonstrate general principles in the functional architecture of the contracting
371   wall of biological pumps and sphincters [60,61]. In contrast to the simplified
372   hypothetical conduits used by Barry [16] and others [60,61], however, the primary
373   wall of a real embryonic heart tube is not of uniform thickness in cross-section (Fig.
374   1A+B). This is the consequence of a non-uniform spatial distribution of the CJ. The
375   original ventral and dorsal midlines of the ventricular tube, – the "fusion" lines of
376   the paired heart fields --, show only a very thin layer of CJ, while marked
377   accumulations of CJ are found along the original left and right lateral walls of the
378   ventricular tube [4,16,37,62-67]. Thus, the CJ of the ventricular tube shows a paired
379   spatial patterning that reflects its origin from the bilaterally paired heart fields. The
380   paired character of CJ distribution is found during all phases of the cardiac cycle. It
381   is particularly prominent, however, at end-systolic occlusion of the endocardial
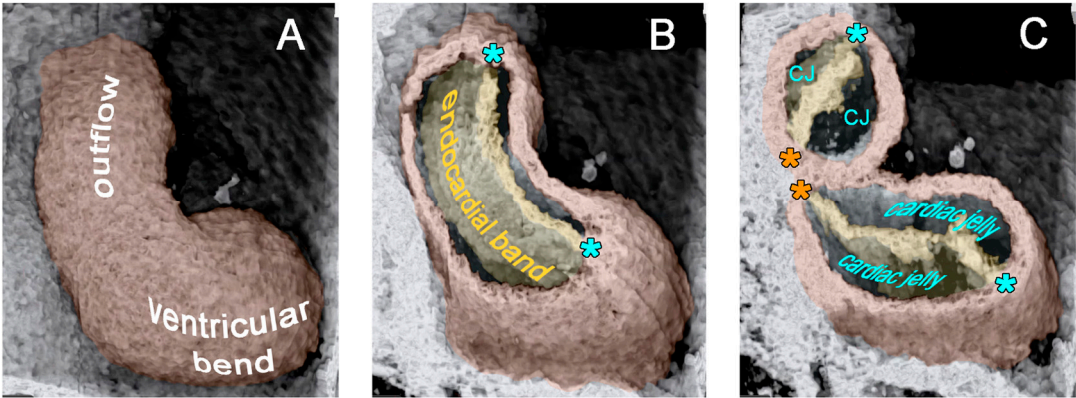382   tube when the CJ has the greatest thickness during the cardiac cycle (Fig. 6).

383   **Figure 6.** These 3D-images, acquired *in vivo* by 4D optical coherence tomography (OCT) [68], show
384   various aspects of the wall architecture of the primary ventricular tube of a HH-stage 12/13 chick
385   embryo heart as seen in right lateral views. Pictures show the ventricular bend and outflow in a fully
386   contracted (end-systolic) state. (**A**) Outer shape of the myocardial tube. (**B**) 3-D shape of the occluded
387   endocardial tube as shown by virtual removal of parts of the myocardial wall. Note that the
388   collapsed endocardial tube has the shape of a flat band, whose edges are fixed to the original ventral
389   and dorsal midlines of the heart tube (marked by blue and orange asterisks, respectively). (**C**)
390   Cross-sections of the ventricular tube at the level of the ventricular bend and outflow as depicted by
391   virtual dissection of OCT datasets. Note that the flattened endocardial tube is flanked by paired
392   accumulations of CJ, which have half-moon shaped cross-sections. The paired character of the
393   CJ-layer reflects the origin of the ventricular tube from the bilaterally paired heart fields.

394   The occluded endocardial tube has the shape of a flat band that marks the original
395   mid-sagittal plane of the heart tube (Fig. 6B). This band is flanked by paired
396   accumulations of thickened CJ, which have half-moon shaped cross-sections.
397   Endocardium and CJ are surrounded by the contracted myocardial wall, which has

398 an elliptic cross-section (Fig. 6C). During the filling phase of the ventricular tube
399 (diastole), the collapsed lumen of the endocardial tube re-expands and acquires an
400 elliptic cross-section flanked by a pair of sickle-shaped accumulations of CJ. The
401 surrounding myocardial wall is in a relaxed state and acquires an almost circular
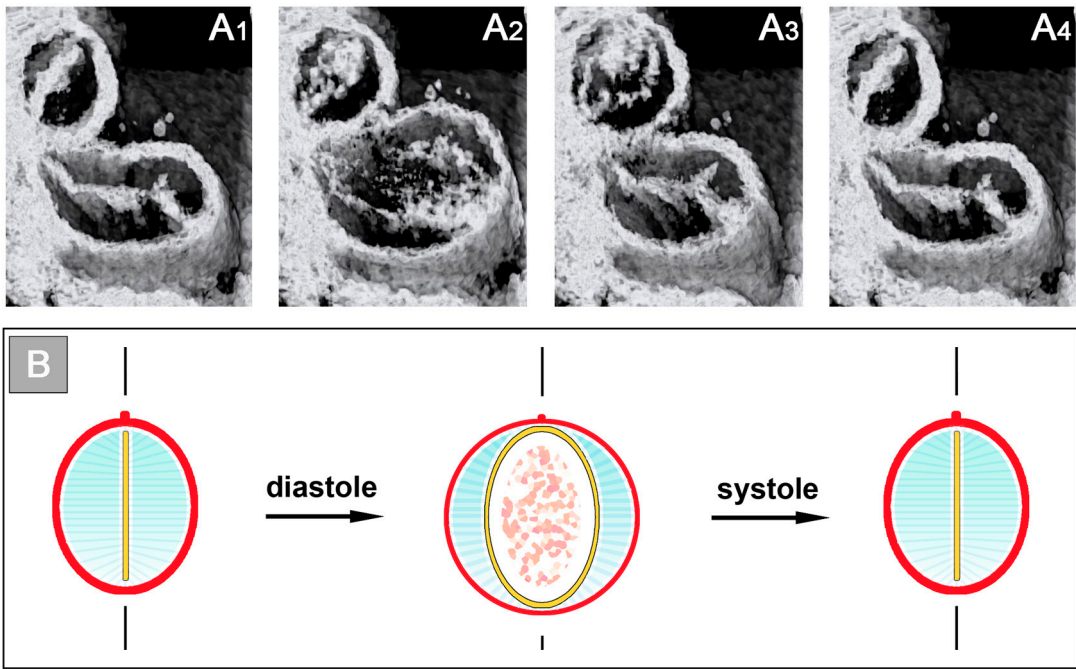402 cross-section (Fig. 7).
403

Figure 7. Cardiac cycle-related changes in cross-sectional shape of the primary ventricular tube as
visualized (**A**) by *in vivo* 4D OCT imaging of a HH-stage 12/13 chick embryo heart (see Fig. 6C); and
shown (**B**) by schematic drawings (same color code as used in Fig. 2). Note that, due to the
non-uniform spatial distribution of the CJ, the endocardial tube does not show concentric widening
and narrowing during the cardiac cycle. The opened endocardial tube has an elliptic cross section,
while the collapsed endocardial tube has a slit-shaped cross section. Note also the cyclic changes in
thickness of the CJ layer. The CJ undergoes thinning during relaxation of the surrounding
myocardial wall (diastole) and thickening during contraction of the myocardial wall (systole).

412   In view of the fact that the non-uniform spatial distribution of CJ reflects the
413 origin of the ventricular tube from bilaterally paired heart fields, it is tempting to
414 suspect that the cross-sectional shape of the primary ventricular tube may represent
415 no more than a functionally insignificant architectural relict of the preceding union
416 of the paired heart fields. Analyses on heart tube models, however, have shown
417 that, compared to a ventricular tube model with circular wall architecture, a
418 ventricular tube model with an elliptic lumen, due to non-uniform CJ distribution,
419 produces a 30% higher area reduction for the same amount of contraction energy
420 introduced into the model system [69]. Thus, the physiologically non-uniform
421 distribution of CJ around the primary ventricular wall can be explained, not only in
422 terms of union of the bilaterally paired heart fields, but additionally in terms of
423 improvement of the mechanical pumping efficiency. Besides solid-dynamic
424 advantages, the non-uniform architecture of the primary ventricular wall may also
425 have fluid-dynamic advantages. Sarin and Mehrotra, for example, have shown that,

426   under certain conditions, the resistance to the flow in a tube of elliptic cross-section
427   can be markedly lower than in a tube of circular cross-section [70]. Future studies
428   are needed to test this idea.
429   The above-mentioned analyses on embryonic heart tube models have shown
430   that the CJ is needed for proper systolic function of the primary ventricular tube.
431   Based on *in vivo* observations on heart tubes of chick embryos, Barry had suggested
432   that the CJ might also support the diastolic filling of the primary ventricular tube
433   [16]. He had observed that, if a HH-stage 11/12 chick embryonic heart tube is
434   transsected caudal to the venous heart pole, coelomic fluid is sucked into the
435   opened heart during the refilling (diastole) phase of the still beating ventricular
436   tube. Sucking motion of the primary ventricular tube may be the dominant filling
437   mechanism during the initial phase of embryonic heart action, since, at HH-stage
438   12, less than 10% of the filling volume of the primary ventricular tube of a chick
439   embryonic heart results from active contraction of the primary atrium [71]. Barry
440   has speculated that the diastolic reopening of the lumen of the primary ventricular
441   tube is powered by the release of passive energy stored in the elastic deformation of
442   compressed CJ during the preceding systole [16]. Besides the statement that the CJ
443   is a resilient substance, however, he did not present any idea about the structural
444   basis for the suspected elastic restoration of the relaxed (diastolic) shape of
445   non-compressed CJ. Thirty years later, however, Nakamura and Manasek
446   attributed the diastolic reopening of the endocardial tube to formed components of
447   the CJ, namely the so-called CJ fibrils [72]. At the time of Barry's pioneering work,
448   the existence of CJ fibrils, as normal histological structures, was questioned by some
449   researchers. At that time, information about the internal architecture of the CJ was
450   obtained only from the examination of routine histological sections of early
451   embryonic heart tubes. In such preparations, fibrillated networks of variable
452   amount and texture are frequently (Fig. 8A), but not regularly (Fig. 1), found within
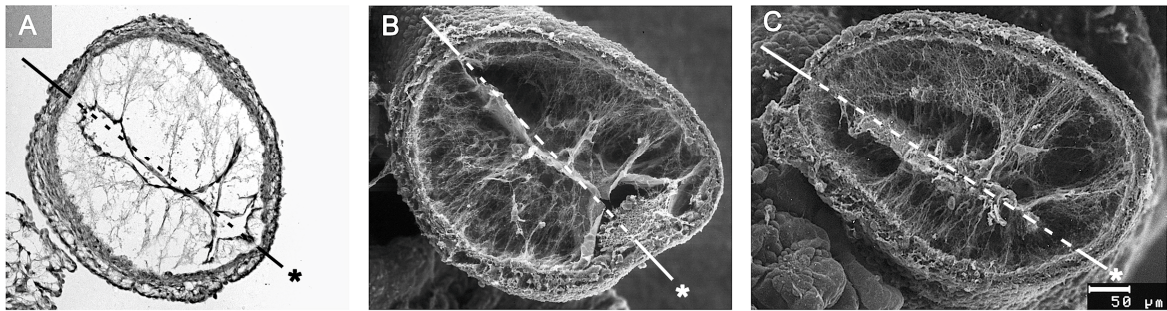453   the myoendocardial space.
454

455   **Figure 8.** These images depict the architecture of the fibrillar components of the CJ as seen on
456   cross-sections of the ventricular tube of embryonic chick hearts (HH-stage 16). (**A**) Routine
457   histological section (HE staining) at the level of the ventricular bend; and (**B**, **C**) scanning electron
458   microscopic pictures of cross-sections at the level of the ventricular bend (B) and ventricular inflow
459   (C). Hearts were fixed at end-systole when the CJ has the greatest thickness during the cardiac cycle.
460   Broken lines mark the closing planes of the collapsed endocardial tubes. Asterisks mark the original
461   ventral midline of the ventricular tube. The CJ fibrils form a delicate network that is anchored to the
462   basal laminae of the primary endocardium and myocardium. Within this network of interconnected

463   fibrils, the principal fiber orientation is perpendicular to the basal surfaces of the endocardial and
464   myocardial tubes. During reopening of the endocardial tube (diastole), the endocardial surfaces
465   curve and the CJ fibrils acquire a principally radial orientation around the center axis of the
466   ventricular tube (not shown).

467   While several investigators regarded these fibrillar networks as normal structural
468   components of the CJ [3,11,52], other investigators interpreted such pictures as
469   showing fixation artifacts, namely the coagula of a principally homogenous ground
470   substance [4,9,27].

471   During the last three decades of the 20th century, several groups analyzed the
472   biochemical nature and/or architecture of CJ fibrils by use of modern microscopic
473   techniques. The generally accepted conclusions arising from these studies are (1)
474   that the fibrillar networks found in the myoendocardial spaces of fixed embryonic
475   heart tubes are normal structural components of the CJ; (2) that the fiber system
476   consists of collagenous as well as non-collagenous filaments; and (3) that the
477   principal orientation of CJ fibrils is perpendicular to the basal surfaces of the
478   primary endocardium and myocardium, which gives the impression of a
479   predominantly radial orientation of the CJ fibrils in diastolic hearts [72-74].

480   With respect to the structural basis of the diastolic CJ function proposed by
481   Barry, Nakamura and Manasek have speculated that, if the radial CJ fibrils are
482   elastic, they should be stretched during systolic thickening of the CJ and thereby
483   store a certain proportion of the myocardial contraction energy. When the
484   myocardial wall relaxes, this energy should be released and drive passive widening
485   of the wall of the primary ventricular tube during diastole [72]. In support of this
486   speculation, they found that radial CJ fibrils appeared to be wavy in relaxed
487   (diastolic) hearts and stretched in contracted (systolic) hearts [72,73]. Besides of the
488   proposed role in diastolic re-expansion of the primary ventricular tube, the CJ fiber
489   system may have further biomechanical functions. Garita and co-workers, for
490   example, have proposed that the system may act as a three-dimensional
491   mechanosensing network used by the primary endocardium and myocardium [67].
492   This idea is in accord with the new conceptual hypothesis that the microfibrillar
493   components of elastic ECMs act as structural tensometers that facilitate cells to
494   sense and respond to changes in tissue mechanics [75].

495   The dynamic behavior of the CJ, described in the hypothetical scenario of
496   Nakamura and Manasek, show striking similarities to the behavior of the ECM of
497   jellyfish during swimming motion. Jellyfish is the informal name given to the
498   medusa-stage of certain soft-bodied marine invertebrates. Jellyfish are mostly
499   free-swimming animals that have a bell- or umbrella-shaped body form. Similar to
500   the situation in the primary ventricular tube of vertebrate embryonic hearts, the soft
501   body of jellyfish is mechanically stabilized by a hydraulic skeleton, made up of a
502   transparent, highly hydrated form of gelatinous ECM. This viscoelastic ECM is
503   called "mesoglea" [23,76]. The mesoglea is interposed between the outer
504   (epidermis) and inner (gastrodermis) skins of the umbrella-shaped body.
505   Corresponding to the CJ, the mesoglea harbors a system of vertically/radially
506   oriented ECM fibers that consists of collagenous as well as non-collagenous

507 components [76-78]. Non-collagenous ECM fibers contribute to the elastic
508 properties of the mesoglea and have been identified as fibrillin-rich fibers [78,79].
509 Jellyfish swim by radial contractions and expansions of their umbrella-shaped
510 bodies. Contraction of the body narrows the lumen of the subumbrellar cavity so
511 that a quantity of its water content is ejected rearward through the opening of the
512 cavity and the animal is propelled forward. During the subsequent expansion of the
513 body, the subumbrellar cavity widens so that water is sucked back into the
514 subumbrellar cavity. Contraction of the jellyfish body is an active process generated
515 by the action of a circular swimming muscle. It is accompanied by a significant
516 increase in thickness of the mesoglea. Expansion, on the other hand, is a passive
517 process driven by the release of energy stored in the elastic deformation of the
518 mesoglea during the preceding contraction. Expansion of the jellyfish body is
519 accompanied by thinning of its mesoglea layer. The elastic restoration of the resting
520 shape of the jellyfish body is mainly attributed to the radially oriented fibers of the
521 mesoglea. These fibers become stretched during contraction-induced thickening of
522 the mesoglea and re-shorten during expansion of the jellyfish body [78,80].

523   The above-mentioned observations on jellyfish suggest that the CJ has a
524 functional design that is widely used in the animal kingdom. We should note,
525 however, that some experimental results seem to cast doubt on the postulated
526 diastolic function of the CJ. Baldwin and co-workers [81] have analyzed the effects
527 of CJ removal (by hyaluronidase treatment) on ventricular function of the
528 post-looped heart tube of rat embryos. They have found that, compared to normal
529 controls, CJ-deficient heart tubes show a significant faster diastolic refilling of the
530 ventricular bend. They have concluded that this finding seems to disprove Barry's
531 concept of a passive, CJ-driven refilling of the primary ventricular tube. We should
532 note here, however, that the higher velocity of diastolic refilling, observed in
533 CJ-deficient heart tubes, can be simply explained by backflow of blood from the
534 aortic sac due to failure of CJ-dependent occlusion of the ventricular outflow
535 portion. The outflow portion normally is in a contracted (systolic) state during
536 refilling (diastole) of the ventricular bend and, thereby, prevents backflow of blood
537 from the aortic sac. We should furthermore note, that the elastic restoration of the
538 relaxed shape of the heart tube, which is proposed to drive diastolic refilling of the
539 heart, can be observed in the beating heart tubes of chick embryos whose
540 cardiovascular systems have been emptied of blood by opening of their vitelline
541 vessels [55].

4. Morphology and Function of the CJ during the Initial Phase of Ventricular Tube Remodeling

544   The primary wall architecture is found along the entire length of the ventricular
545 tube only during a relatively short phase of early cardiac pumping action. In chick
546 embryos, this phase spans the developmental period from HH-stage 10/11 to
547 HH-stage 12/13, and in human embryos it spans the developmental period defined
548 by Carnegie stage 10. Subsequent to the establishment of a hemodynamically
549 effective pulsatile blood flow, a remodeling process starts within the ventricular

550 tube that transforms its primary wall architecture. During the initial phase of
551 ventricular tube remodeling, changes in the wall architecture are confined to the
552 endocardial tube and CJ along the outer curvature (convexity) of the ventricular
553 bend. The wall of the inner curvature (concavity) of the ventricular bend as well as
554 the walls of the ventricular inflow and outflow portions do not show significant
555 changes of their primary architecture. This remodeling pattern corresponds to the
556 spatial distribution of high (inflow, inner curvature, outflow) and low (outer
557 curvature) shear stress areas found within the endocardium of the looped
558 ventricular tube of chick embryos [82], suggesting that hemodynamic forces may
559 trigger the remodeling process.
560   Remodeling starts with the formation of multiple sprout- or pouch-like
561 outgrowths of the endocardial tube that invade the CJ and grow toward the basal
562 layer of the myocardium [4,6,53-55]. Scanning electron microscopic data from chick
563 embryos disclosed an intimate physical connection between the endocardial
564 sprouts and the radially oriented CJ fibers, suggesting that the latter might be used
565 as guidance by the former [55].
566   Concomitant with the outgrowth of endocardial sprouts, the thickness of the CJ
567 layer is reduced along the outer curvature of the ventricular bend and the tips of the
568 endocardial sprouts eventually come into direct contact with the basal surface of
569 the myocardium. These endocardial-myocardial contacts are established exactly in
570 those areas where the myocardial wall will expand and develop a trabeculated
571 architecture during the subsequent phase of advanced ventricular tube remodeling.
572 Davis and Streeter, therefore, called the endocardial outgrowths the "primordia of
573 endothelial trabeculae" [4,6]. In chick embryos, the initial phase of ventricular tube
574 remodeling spans the developmental period from HH-stage 13 to HH-stage 16/17,
575 and in human embryos it spans the developmental period defined by Carnegie
576 stage 11.
577   The invasion of multiple endocardial protrusions into the CJ leads to
578 establishment of two broad areas of diminished CJ along the outer curvature of the
579 ventricular bend, which mark the positions of the prospective apical trabeculated
580 regions of the left and right ventricles. In the following, these areas will be termed
581 "trabecular shields". Comparison of data from human and chick embryos disclose
582 species-specific differences in the chronology of the establishment of the trabecular
583 shields. In human embryos, the formation of trabecular shields starts at the level of
584 the prospective left ventricle [6], while in chick embryos, this process starts at the
585 level of the prospective right ventricle [83,84]. These differences may reflect
586 species-specific differences in the chronology of union of the bilateral heart fields.
587 In mammalian embryos, union of the heart fields starts at the level of the
588 prospective apical trabeculated regions of the left ventricle [41], while in chick
589 embryos this process is said to start at the level of the prospective apical
590 trabeculated region of the right ventricle [85].
591   Historical descriptions do not mention any internal patterning of the trabecular
592 shields. However, our studies on chick embryos have shown that these areas have a
593 regular spatial patterning that is best visualized by three-dimensional imaging of

594   the outer shape of the collapsed (systolic) endocardial tube (Figs. 9). This pattern is
595   also found on historical pictures from human embryonic heart tubes (Fig. 10) but,
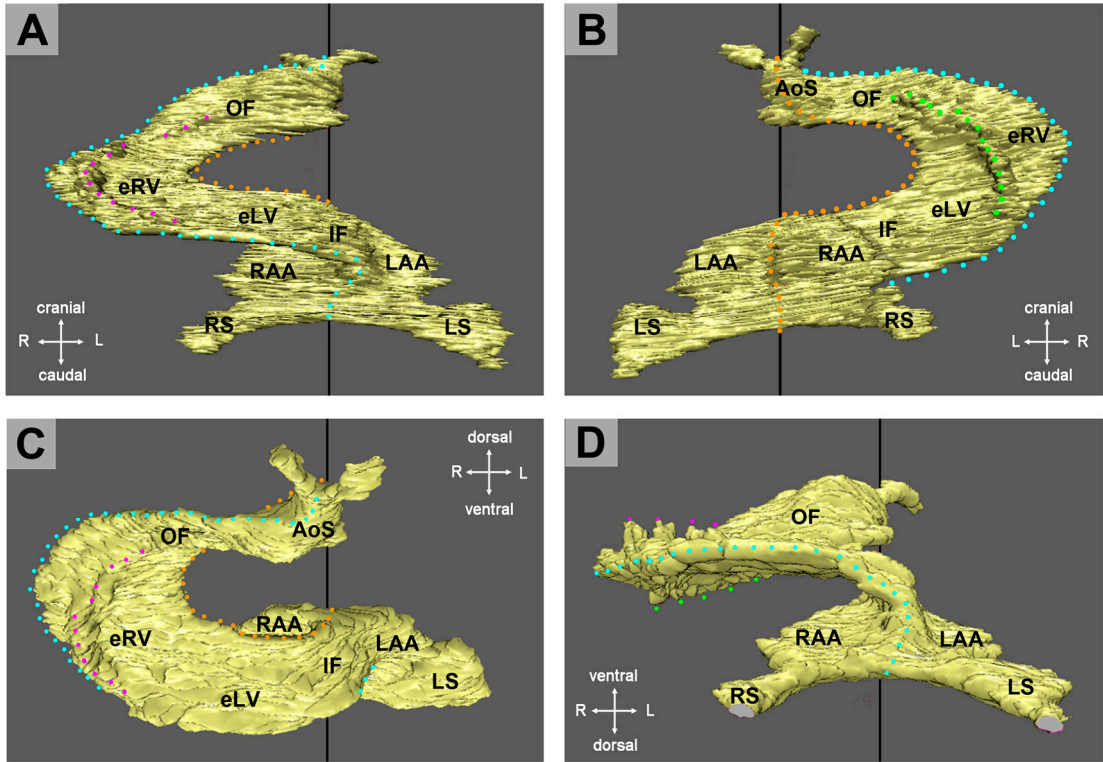596   for unknown reasons, has escaped the attention of previous investigators.
597

598   **Figure 9.** These pictures show the outer shape of an occluded endocardial tube of an embryonic chick
599   heart during the initial phase of ventricular tube remodeling (HH-stage 14). Images were generated
600   by virtual 3-D reconstructions of OCT data sets from a heart that has been fixed in an artificially
601   induced general contraction. (**A**) Frontal view. (**B**) Dorsal view. (**C**) Cranial view. (**D**) Caudal view.
602   The outer curvature of the ventricular bend has a folded surface, which is characterized by three
603   folds: (1) a midline fold that corresponds to the original ventral edge of the occluded endocardial
604   tube (marked by lines of blue dots). This fold subdivides the trabecular shields into two halves. (2+3)
605   A pair of lateral folds that form the lateral borders of the trabecular shields (marked by dotted lines
606   in magenta and green). Abbreviations: eLV = embryonic left ventricle; eRV = embryonic right
607   ventricle; IF = inflow portion of ventricular tube; RAA = anlage of right atrial appendage; RS = right
608   horn of sinus venosus; LS = left horn of sinus venosus; OF = outflow portion of ventricular tube.
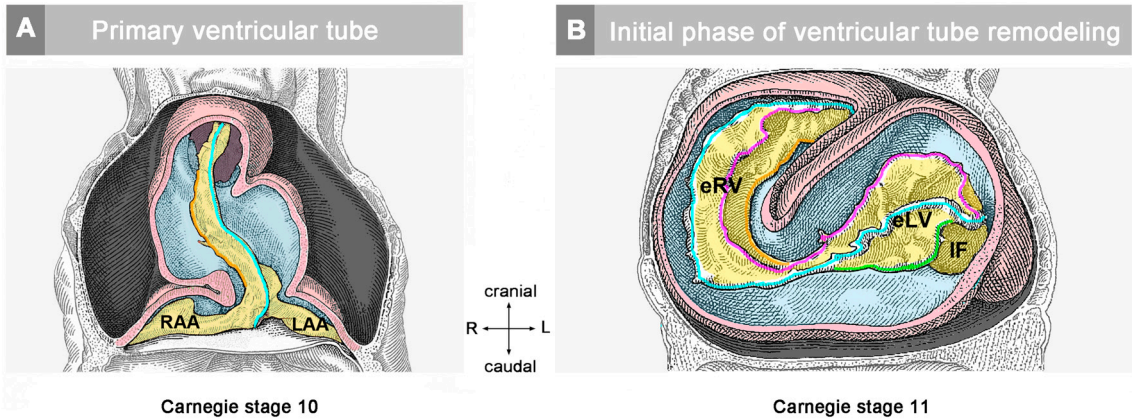
Figure 10. These drawings depict the changes in the outer shape of the occluded (systolic) endocardial tube of human embryonic heart tubes during the initial phase of ventricular tube remodeling. Hearts are shown in frontal views within the opened pericardial cavities. The ventral myocardial walls have been removed to facilitate views on the endocardial tubes. (**A**) The occlude endocardial tube of the primary ventricular tube has the shape of a flat band. Its ventral (blue line) and dorsal (orange line) edges correspond to the original ventral and dorsal midlines of the heart. (**B**) Due to the formation of trabecular shields, the occluded endocardial tube has a folded surface along its outer curvature. Corresponding to the situation in chick embryonic hearts (Fig. 9), the picture is dominated by the presence of three folds: (1) a midline fold that corresponds to the original ventral edge of the occluded endocardial tube (blue line). This fold subdivides the trabecular shields into two halves. (2+3) A pair of lateral folds that form the lateral borders of the trabecular shields (magenta and green lines). Drawings are based on Figures 22 and 26 from Davis [4]. Same abbreviations as used in Figure 9.

As already described, the collapsed endocardial tube of the primary ventricular tube has the shape of a flat band whose edges correspond to the original ventral and dorsal midlines of the heart tube (Figs. 6B + 10A). Due to the formation of the trabecular shields, the outer shape of the collapsed endocardial tube of the ventricular bend no longer appears as a flat band but shows a folded surface along its outer curvature (Figs. 9 and 10B). The picture is dominated by the presence of three regularly formed folds. The first of these folds corresponds to the original ventral (midline) edge of the flattened primary endocardial tube. It subdivides the trabecular shields into two halves, which occupy the outer curvatures of the original left and right halves of the ventricular tube, respectively. The remaining two folds form the lateral borders of the trabecular shields. Based on this finding, it becomes apparent that each trabecular shield is a bilaterally paired structure.

The functional significance of early ventricular wall remodeling has not been clarified up to now. It is evident that the formation of the trabecular shields leads to an increase of the end-diastolic volume of the endocardial tube of the ventricular bend. This might support the pumping function. An argument against this idea may be the fact that the increase in end-diastolic volume is at the expense of the CJ layer. Since a thick layer of CJ is needed for complete end-systolic occlusion of the endocardial tube, it is tempting to speculate that the formation of the trabecular shields might prevent complete end-systolic occlusion of the endocardial lumen and thereby reduces the original 100% ejection fraction. This might mitigate the positive effects of early ventricular wall remodeling. However, *in vivo* OCT imaging

644   of the cardiac cycle of embryonic chick hearts has shown that, due to the
645   above-mentioned system of endocardial folds, the endocardial lumen of the
646   ventricular bend still undergoes complete end-systolic occlusion [55]. The cross
647   section of the collapsed endocardial tube is no longer slit-shaped but has the shape
648   of a latin cross. The descending arm of this cross corresponds to the closure plane of
649   the primary endocardial tube while the horizontal arms represent the closure
650   planes of the lateral folds. During diastolic refilling of the ventricular bend, the
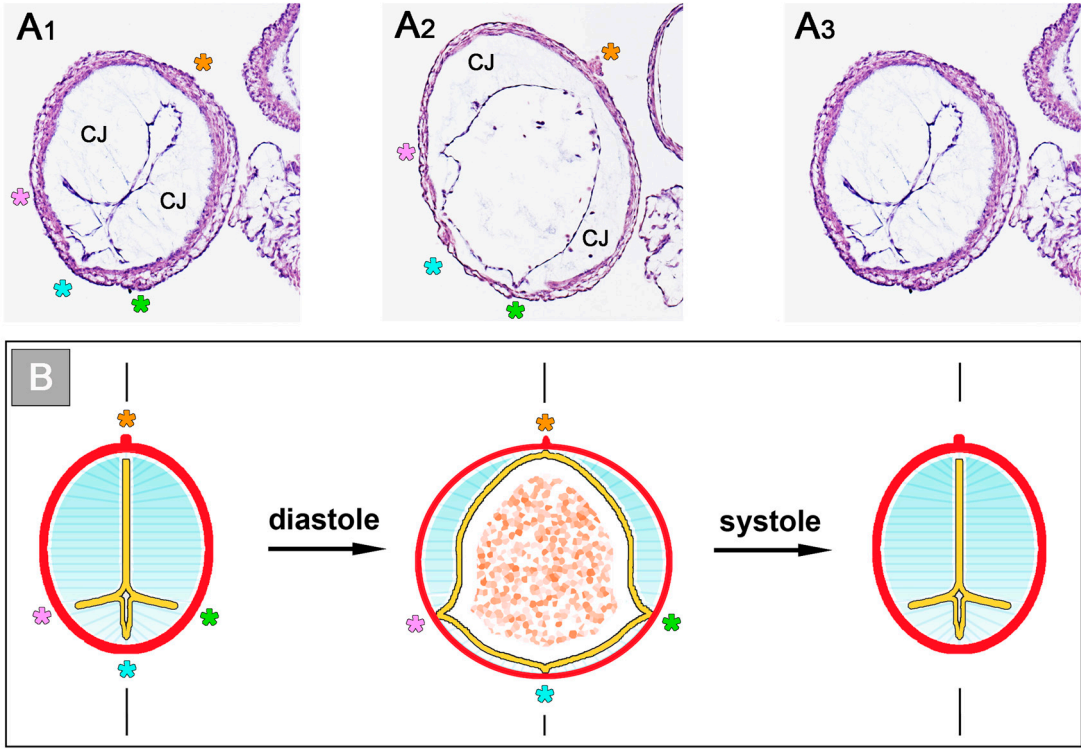651   endocardial tube acquires a bell-shaped or deltoid cross section. (Fig. 11).
652

653   **Figure 11.** Initial phase of ventricular tube remodeling. Cardiac cycle-related changes in
654   cross-sectional shape of the ventricular bend as illustrated (**A**) by histological sections of HH-stage 16
655   chick embryonic hearts, which have been fixed in emptied (A1, A3) and filled (A2) states; and shown
656   (**B**) by schematic drawings (same color code as used in Fig. 2). Asterisks mark the original ventral
657   (light blue) and dorsal (orange) midlines of the heart as well as the lateral borders of the trabecular
658   shields (magenta and green). Note that, due to formation of the trabecular shield, the opened
659   endocardial tube has a bell-shaped or deltoid cross section, while the cross section of the collapsed
660   endocardial tube has the shape of a latin cross. Note also the cyclic changes in thickness of the CJ
661   layer.

662   The above-mentioned studies of Taber and Perrucchio [69] have shown that the
663   mechanical pumping efficiency of the early embryonic heart tube depends on the
664   cross-sectional shape of its endocardial tube. Compared to a tube of circular inner
665   cross section, the natural design of a ventricular tube of elliptic inner cross section
666   was found to work at a higher mechanical efficiency. Early ventricular tube
667   remodeling transforms the initially elliptic cross section of the opened endocardial
668   tube of the ventricular bend into a deltoid cross section. At the present time, we do

669 not know whether this transformation has any relevance for the pumping efficiency
670 of the ventricular bend. We should note, however, that this shape change is
671 accompanied by a general increase in the pumping performance of the embryonic
672 heart tube [86]. Future studies are needed to clarify the relationships between the
673 deltoid cross section and the pumping efficiency and hemodynamics of the
674 ventricular bend.

675 Our reflections on the functional significance of the morphological dynamics of
676 the ventricular bend would not be complete without referring to a peculiar
677 phenomenon, which we have called "end-systolic stretching" [55]. Our data from *in*
678 *vivo* imaging of the pump action of the ventricular bend of embryonic chick hearts
679 have shown that the systolic deformations of the shape of the ventricular tube do
680 not stop with the contact of opposing luminal surfaces of the emptied endocardial
681 tube. Subsequent to end-systolic occlusion of the endocardial lumen, the ventricular
682 wall becomes stretched along its original dorso-ventral axis, so that its outer
683 cross-sectional shape becomes transformed from a circle into an oval (Fig. 12). It is
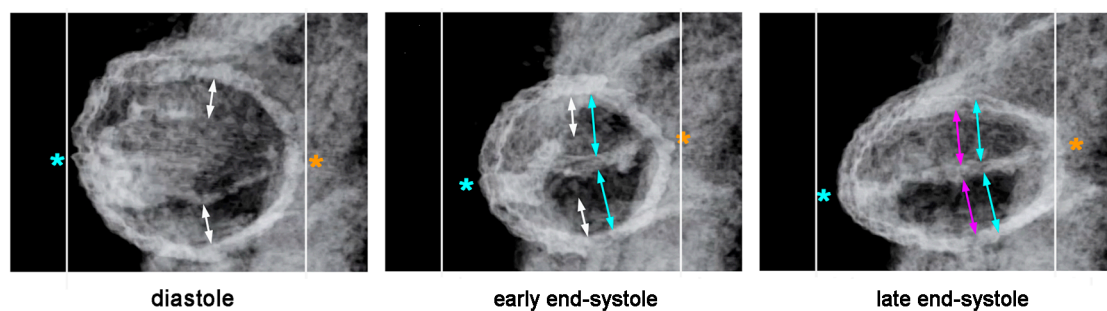684 evident that this shape change is driven by end-systolic deformation of CJ.

685

diastole   early end-systole   late end-systole

686 **Figure 12.** These images obtained by 4-dimensional *in vivo* OCT imaging of a HH-stage 15 embryonic
687 chick heart depict the peculiar phenomenon of end-systolic stretching of the cross section of the
688 ventricular bend along the original dorso-ventral axis. Asterisks mark the original ventral (light blue)
689 and dorsal (orange) midlines, which are found along the outer and inner curvatures of the
690 ventricular bend, respectively. Note the striking increase in thickness of the CJ layer between diastole
691 and early end-systole (indicated by white and blue arrows). Late end-systolic stretching of the cross
692 section of the ventricular bend leads to a slight decrease in CJ thickness (compare blue and magenta
693 arrows). White lines mark the diastolic length of the original dorso-ventral axis.

694 The phenomenon of end-systolic stretching, therefore, confirms Barry's statement
695 that the myocardial contraction energy is used not only for propulsion of blood but
696 additionally for the elastic deformation of the CJ layer. End-systolic stretching is
697 most prominent at the level of the ventricular bend and during the initial phase of
698 ventricular tube remodeling [55]. This observation not only suggests that the
699 ventricular bend generates the strongest contraction force of all portions of the
700 ventricular tube, but additionally may generate the highest proportion of the
701 proposed sucking action of the ventricular tube.

702 **5. Morphology and Function of the CJ during the Advanced Phase of Ventricular**
703 **Tube Remodeling (Trabeculation, Ballooning, Endocardial Cushions/Ridges)**

704　　　The time point of transition from the initial to advanced phase of ventricular
705　tube remodeling is reached when the endocardial projections of the trabecular
706　shields have established direct contacts to the basal myocardial surface of the outer
707　curvature of the ventricular bend. The capillary-like endocardial projections now
708　penetrate the compact basal layer of the myocardium, invade the intercellular
709　spaces of the loosely arranged middle (reticular) layer of the myocardial wall (Fig.
710　5A), and start establishment of a primitive blood supply to the developing
711　myocardium [87]. The affected areas of the myocardial wall thereby loose their
712　originally smooth basal surface and start formation of a sponge-like inner layer
713　whose muscular network is in intimate contact with branches of the endocardial
714　projections. The sponge-like myocardium consists of myocardial trabeculations and
715　intertrabecular spaces [53,54,87]. The intertrabecular spaces are occupied by the
716　capillary-like endocardial projections, which traditionally have been named
717　"endocardial trabeculations" [4,6,88] or "myocardial sinusoids" [89,90].

718　　　The formation of the trabecular layer of the ventricular myocardium is
719　accompanied by centrifugal growth of the affected areas. When seen from the
720　outside, this growth process leads to formation of aneurym- or balloon-like
721　expansions of the ventricular tube along its outer curvature [56,88]. Consequently,
722　this myocardial growth process was named ventricular "ballooning" [56]. The
723　ballooning portions of the ventricular bend are the first externally visible
724　manifestations of the prospective left and right ventricle, and, therefore, are named
725　the embryonic left and right ventricle, respectively. In chick embryos, the formation
726　of myocardial trabeculae starts at HH-stage 17 [54,83,91], and in human embryos it
727　starts at Carnegie stage 12 [39,88].

728　　　The embryonic ventricles have lost the originally thick CJ layer and the original
729　tubular shape of the ventricular bend. This is in contrast to the inflow and outflow
730　portions, which still preserve the original tubular shape and still possess a thick
731　myoendocardial tissue layer. Consequently, the inflow and outflow portions now
732　have visible anatomical borders at their upstream and downstream ends. They have
733　become anatomically well-demarcated units, which are named the
734　"atrio-ventricular canal" (AVC) and "outflow tract" (OFT), respectively. The CJ of
735　the AVC and OFT becomes populated by endocardium-derived mesenchymal cells
736　and, thereby, looses its cell-free phenotype (Fig. 5B) and changes its biophysical
737　properties (e.g. stiffness) [27,57,58]. The paired accumulations of cellularized CJ are
738　named endocardial cushions (in the AVC) or endocardial ridges (in the OFT).

739　　　The above-mentioned changes in the anatomy of the developing heart are
740　accompanied by changes in the pumping behavior of the primary ventricular tube
741　derivatives. The balloon-shaped embryonic ventricles become the main pumping
742　units of the developing heart and develop the mature patterns of electrical
743　activation and contraction [92,93]. The AVC and OFT on the other hand act as
744　tubular conduits, which (1) connect the embryonic ventricles with the developing
745　atria and aortic sac, respectively; and (2) control intracardiac blood flow by opening
746　and closure of their lumen. The latter function of the AVC and OFT is based on a

747 sphincter-like action and has the same effects on blood flow as the mature heart
748 valves.
749   During the past decades, several excellent review articles have dealt with the
750 above-mentioned processes of ventricular trabeculation/ballooning [94-96] and
751 endocardial cushions/ridges development [58,97,98]. We, therefore, do not want to
752 add a further extensive review about these processes in the present article.
753 However, we think that there exist a few facts that are worth mentioning if we want
754 to understand the relation between the CJ and the formation of endocardial
755 cushions/ridges and myocardial trabeculations.

5.1. Notes on Morphology and Function of Endocardial Cushions/Ridges

757   With respect to the relation between CJ and endocardial cushions/ridges we
758 want to highlight the following facts: (1) Endocardial cushions/ridges arise from
759 remodeling of the non-removed CJ of the inflow and outflow portions of the
760 primary ventricular tube [27]. They do not represent de novo formations. (2) The
761 paired occurrence of endocardial cushions/ridges is based on the non-uniform
762 spatial distribution of the CJ in the primary ventricular tube and, therefore, reflects
763 the bilaterally paired origin of the whole heart. Thus, endocardial cushions/ridges
764 are paired structures whose partners can be assigned to the original left and right
765 halves of the straight ventricular tube, respectively [62,100-102]. (3) Endocardial
766 cushions/ridges principally fulfill the same function as the CJ [27]. They act as
767 passive filler tissues that facilitate complete occlusion of the endocardial lumen of
768 the AVC and OFT during contraction of the myocardial wall. Their architecture and
769 biomechanical properties are adapted to the increasing hemodynamic loads of the
770 developing heart at late looping- and early post-looping stages [58]. (4) It is
771 frequently stated that CJ and endocardial cushions/ridges control blood flow by a
772 valve-like action [e.g. 27,103]. We think that such a description may hamper
773 understanding of the pumping function of the valveless embryonic heart since it
774 does not correctly reflect reality. The mature heart valves are biological devices that
775 open and close the cardiac flow pathways in a purely passive manner driven by
776 differences in blood pressure along the flow pathways. The basis for this behavior is
777 the form design of heart valves, which normally permits one-way flow, only. This
778 behavior is in sharp contrast to the action of the endocardial cushions/ridges. These
779 biological devices do not open and close the endocardial lumen in a passive, blood
780 pressure-driven way. Closure of the endocardial lumen of the AVC and OFT is an
781 active process that is driven by contraction of the surrounding myocardial wall.
782 During contraction of the myocardial wall, the endocardial cushions/ridges act as
783 passive filler tissues facilitating complete occlusion of the endocardial lumen.
784 Reopening of the lumen depends on relaxation of the myocardial wall.
785 Furthermore, the form design of endocardial cushions does not determine the flow
786 direction in the valveless embryonic heart. Instead, the flow direction is determined
787 by the sequential contractions of the developing atrial and ventricular heart
788 chambers. If the normal pattern of heart beat propagation is reversed, the flow
789 direction is also reversed [104]. Such a behavior, as well as the wall architecture of

790   the AVC and OFT, corresponds to biological sphincters [61]. We, therefore, think
791   that the correct functional description of the action of the AVC and OFT is that of a
792   sphincter-like action. This has been done previously by some investigators
793   [94,105-108] but, for unknown reasons, did not receive general acceptance.

794   *5.2. Notes on Ventricular Trabeculation and Ballooning*

795   With respect to the relation between CJ and the formation of ventricular
796   trabeculations we want to comment on two aspects. The first is the mechanism of
797   formation of myocardial trabeculations and the second is the ballooning model.

798   The hearts of CJ-deficient mouse embryos do not form a trabeculated wall
799   architecture suggesting that the process of ventricular trabeculation depends on the
800   presence of CJ [109]. The functional interpretation of this finding is made difficult
801   by the fact that in the literature two opposing concepts exist about the
802   morphogenetic mechanism driving the formation of the trabeculated layer of the
803   ventricular myocardium of vertebrate embryonic hearts. The first of these concepts
804   corresponds to the description of the trabeculation process given in the preceding
805   paragraphs of our present review article (Figs. 4C and 5A). It describes the
806   formation and expansion of the trabecular layer of the embryonic ventricles as a
807   centrifugal growth process [6,53,54,56,83,88,105,110]. This means that the
808   myocardial trabeculae and the sprout-like endocardial projections principally
809   elongate by outward growth toward the pericardial surface of the ventricular wall.
810   The innermost portions of the trabeculated myocardium -- the free edges of
811   myocardial trabeculae -- are regarded as remnants of the original basal layer of the
812   primary myocardium, which do not significantly change their original positional
813   relationship to the tube-shaped remainders of the primary ventricular tube (AVC
814   and OFT). This concept is founded on morphological data, which show that the free
815   edges of the myocardial trabeculae form an imaginary line that follows the original
816   course of the myocardial wall of the outer curvature of the primary ventricular tube
817   (Fig. 13) [6,83,88,105,110]. It is furthermore supported by experimental and
818   molecular data suggesting that the edges of the myocardial trabeculae harbor the
819   ontogenetically oldest cells directly derived from the myocardium of the primary
820   ventricular tube [94].
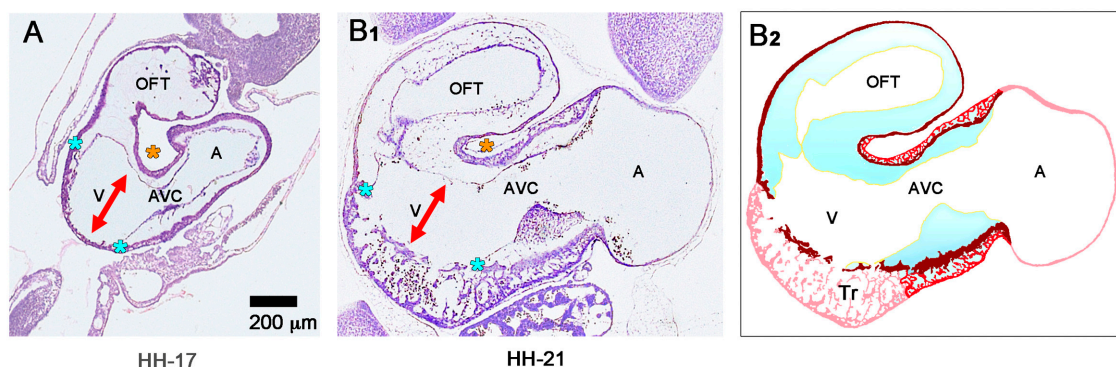
821

Figure 13. These histological sections from embryonic chick hearts depict the changes in ventricular wall architecture during the advanced phase of ventricular tube remodeling. (**A**) At the time point of transition from the initial to advanced phase of ventricular tube remodeling (HH-stage 16/17), the outer curvature of the ventricular bend lacks a CJ layer and the tips of the endocardial projections of the trabecular shields are in direct contact to the basal layer of the ventricular myocardium (blue asterisks mark the proximal and distal borders of the trabecular shields; orange asterisk mark the inner curvature of the ventricular bend). In the AVC, endocardium-derived mesenchyme has started invasion of the CJ. Note that the myocardial walls of all portions of the primary ventricular tube have a tubular shape. (**B1 + B2**) HH-stage 21. Due to the formation of trabeculated embryonic ventricles, the outer contour of the ventricular bend has lost its original tubular shape. The AVC and OFT have preserved their original tubular shapes. When looking on the inner structure of the embryonic ventricles, however, it becomes apparent that the original tubular shape of the ventricular bend is still visible if one follows an imaginary line that connects the free edges of the myocardial trabeculae (highlighted by dark red color in **B2**). Note that the free lumen of the embryonic ventricles does not change significantly between HH-stages 17 and 21. Note also the structural similarity between the non-trabeculated, three-layered myocardium of the AVC (inner compact layer, reticular layer, outer compact layer) and the trabeculated myocardium of the embryonic ventricles. Color code used in B2: dark red = remnants of the primary ventricular myocardium; red = reticular and outer compact myocardium of the AVC; light red = trabeculated and outer compact myocardium of embryonic ventricles, and atrial myocardium; light blue = CJ and intramyocardial ECM; yellow = endocardium. Abbreviations: A = primary atrium; AVC = atrio-ventricular canal; OFT = outflow tract; Tr = trabecular layer of ventricular myocardium; V = free lumen of the primary ventricular tube.

The second concept of formation of myocardial trabeculae describes the emergence and expansion of the trabecular layer of the embryonic ventricles as a centripetal growth process [95,108,111,113]. This means that the myocardial trabeculae are suspected to elongate by inward growth toward the centers of the embryonic ventricles (see Fig. 3 in [95], Fig. 3 in [111], and Fig. 1 in [112]). This inward growth is suspected to result either from a buckling process [95] or from the translocation of ventricular cardiomyocytes (by directional cell migration and oriented cell divisions) into non-removed CJ between the endocardial projections of the trabecular shields [reviewed by Wu 2018]. The latter mechanistic concept suggests that the CJ might act as a physical route for the ingrowth of myocardial trabeculae. This idea could nicely explain the above-mentioned observation that CJ-deficient hearts do not form myocardial trabeculae [109]. We should note, however, that the inward growth concept conflicts with the morphological situation found in higher vertebrate embryos. If myocardial trabeculae would preferentially elongate by inward growth toward the centers of the embryonic ventricles, we should expect that the free lumen of the embryonic ventricles become continuously narrowed by the growing trabeculae (see schematic drawing in [112]). As shown in our figure 13, however, the diameter of the free ventricular lumen does not change significantly during the emergence of ventricular trabeculations.

In view of the arguments outlined above, it becomes apparent that we favor the centrifugal growth concept of myocardial trabeculations. With respect to the phenotype of CJ-deficient embryonic hearts, we should note that such hearts not only lack the CJ layer. They, additionally, show the abnormal phenotype of a multilayered compact myocardium that lacks any trace of reticular myocardium (see Fig. 4 in [109]). Prior to the emergence of myocardial trabeculae, the ventricular

869 myocardium normally thickens by the formation of an ECM-rich reticular layer,
870 which is sandwiched between its outer (apical) and inner (basal) compact layers
871 (Fig. 5A). The absence of reticular myocardium shows that CJ-deficient hearts not
872 only lack the myoendocardial ECM compartment (= CJ). They additionally lack the
873 frequently neglected second ECM compartment of early embryonic hearts, namely
874 the intramyocardial ECM. In view of this finding, the question arises as to whether
875 the absence of myocardial trabeculae, found in cases of CJ-deficient hearts, might be
876 explained by the absence of intramyocardial ECM rather than the absence of CJ. It is
877 evident that the establishment of a reticular arrangement of cardiomyocytes
878 depends on the production of intramyocardial ECM. We speculate that the
879 production of intramyocardial ECM not only facilitates the formation of the
880 reticular layer myocardium but, additionally, facilitates the invasion of the
881 endocardial projections into the ventricular myocardial wall, which eventually
882 transforms the reticular myocardium into the so-called trabeculated myocardium.

883   We finally want to comment on the relation between CJ morphogenesis and the
884 ballooning model for cardiac chamber formation, which was introduced by the
885 Amsterdam group in 2000 [56]. The ballooning model distinguishes four solitary
886 ballooning centers that form along the outer curvatures of the primary atrium and
887 primary ventricular tube. These centers are: (1) a right- and (2) a left-sided atrial
888 center, which give rise to the atrial appendages of the prospective right and left
889 atrium, respectively; and (3) a proximal and (4) a distal ventricular center, which
890 give rise to the apical trabeculated regions of the prospective left and right ventricle,
891 respectively. We principally agree with this elegant model, which is based on
892 profound morphological as well as molecular data. Based on our present
893 knowledge about the morphogenesis of the CJ, however, we come to a slightly
894 modified concept of chamber ballooning that emphasizes the bilaterally paired
895 origin of the heart. In the preceding sections of our review article, we have shown
896 that the formation and remodeling of the CJ run in bilaterally paired patterns. The
897 CJ of the primary ventricular tube has a non-uniform spatial distribution that
898 reflects its origin from the left- and right-sided heart fields. The endocardial
899 cushions/ridges are bilaterally paired structures, and the outgrowth of endocardial
900 sprouts/projections into the CJ of the outer curvature of the ventricular bend runs in
901 a bilaterally paired pattern. We have furthermore shown that the latter process does
902 not stop at the basal surface of the myocardium. The endocardial
903 sprouts/projections of the trabecular shields invade the myocardial wall and
904 contribute to trabeculation and ventricular chamber ballooning. It is, therefore,
905 tempting to speculate that the latter two processes might start in a bilaterally paired
906 fashion. During a recent project on heart looping morphogenesis, which was
907 conducted in the lab of one of us (J.M.), we found support for this idea. Scanning
908 electron microscopic analyzes of the outer shape changes of early embryonic mouse
909 hearts have shown that the initial step of externally visible ventricular chamber
910 ballooning is indeed characterized by the emergence of two half-balloons that
911 expand toward the original ventro-lateral walls of the primary ventricular tube. The
912 ventral wall of the outer curvature of the ventricular bend does not significantly

913   participate in this early step of chamber ballooning (Fig. 14A). With continuing
914   expansion of the paired half-balloons, however, the ventral wall of the outer
915   curvature becomes successively incorporated into the ballooning process so that the
916   initially separated ballooning centers eventually merge to a single unit (Fig. 14B,C).
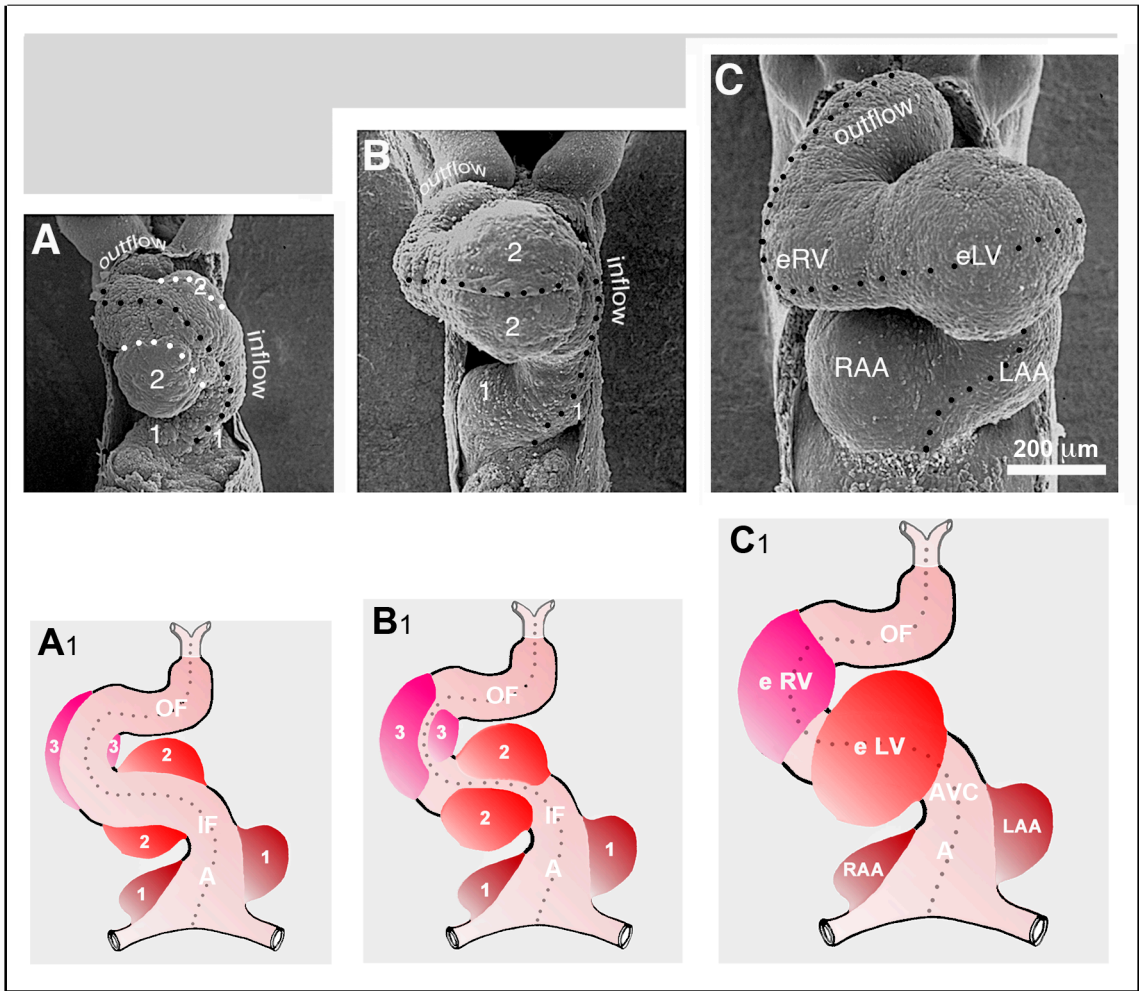917

918   **Figure 14.** The modified model of cardiac chamber ballooning as depicted by changes in the outer
919   shape of early embryonic hearts. (**A–C**) Scanning electron micrographs of embryonic mouse hearts
920   on ED 8.5 (A), ED 9.0 (B), and ED 9.75 (C). Hearts are shown in fronto-caudal views. This facilitates
921   direct imaging of the surface of the outer curvature of the ventricular bend. The black dotted lines
922   mark the original ventral midline of the heart. Note that the inner curvature is not visible. (**A1–C1**)
923   Schematic illustrations of the situations shown in Figs. A-C. (**A, A1**) The initial steps of externally
924   visible chamber ballooning are characterized by the emergence of bilaterally paired ballooning
925   centers at three levels: (1) the embryonic atrium, (2) the prospective left ventricle, and (3) the
926   prospective right ventricle. The white dotted lines in Fig. A mark the ventral borders between the
927   remnant of the primary ventricular tube and the paired ballooning centers of the prospective left
928   ventricle. (**B, B1**) Due to expansion of the paired ballooning centers of the prospective ventricles,
929   their ventral borders shift toward the original ventral midline of the ventricular bend. (**C, C1**) The
930   originally paired ballooning centers of the prospective ventricles unite to form single units
931   (embryonic left and right ventricle) that give rise to the apical trabeculated regions of the prospective
932   ventricles. The paired ballooning centers of the embryonic atrium remain separated and give rise to
933   the atrial appendages of the mature heart. Same abbreviations as used in Figure 9.

The initially paired character of the emergence of externally visible embryonic heart chambers seems to correspond to the spatial patterns of myocardial proliferative activity that have been documented during early chamber formation of chick and human embryonic hearts [see Fig. 7B in 114, and Fig. 3H in 115].

In view of the observations described above, we have developed a modified concept of early heart chamber ballooning that distinguishes three primarily paired ballooning centers (Fig. 14A1-C1). These three centers form at the level of the primary atrium, the level of the proximal portion of the ventricular bend and the level of the distal portion of the ventricular bend. Each of these centers consists of one partner that derives from the left-sided heart field and another partner that derives from the right-sided heart field. The partners of the proximal and distal ventricular ballooning centers normally merge to form single units, which are called the embryonic left and right ventricle, respectively. These units give rise to the apical trabeculated regions of the prospective left and right ventricle, respectively. The partners of the atrial ballooning center remain separated and give rise to the atrial appendages of the prospective right and left atrium, respectively.

Author Contributions: J.M. and M.Y. conceived the paper; M.Y. contributed *in vivo* OCT imaging data; J.M. contributed histological and scanning electron microscopic data, as well as ex vivo OCT imaging data; J.M. and M.Y. analyzed the imaging data; J.M. made the artwork and wrote the first draft of the paper; J.M. and M.Y. carefully edited the final version of the manuscript.

Conflicts of Interest: The authors declare no conflict of interest.

References

1. Männer J.; Wessel A.; Yelbuz T.M. How does the tubular embryonic heart work? Looking for the physical mechanism driving unidirectional blood flow in the valveless embryonic heart tube. *Dev Dyn* **2010**, *239*, 1035-1046.
2. Moorman, A.FM.; Lamers, W.H. Molecular anatomy of the developing heart. *Trends Cardiovasc Med* **1994**, *4*, 257-264.
3. Ingalls, N.W. A human embryo at the beginning of segmentation, with special reference to the vascular system. *Contr Embryol Carneg Instn* **1920**, *11*, 61-90.
4. Davis, C.L. The development of the human heart from its first appearance to the stage found in embryos of twenty paired somites. *Carnegie Inst Wash, Publ 380, Contr Embryol* **1927**, 19, 245-284.
5. Streeter, G.L. Developmental horizons in human embryos. Description of age group XIII, embryos about 4 or 5 millimeters long, and age group XIV, period of indentation of the lens vesicle. *Carnegie Inst Wash, Publ 557, Contrib Embryol* **1945**, 31:29-63.
6. Streeter, G.L. Developmental horizons in human embryos. Description of age groups XV, XVI, XVII, and XVIII, being the third issue of a survey of the Carnegie Collection. *Carnegie Inst Wash, Publ 575, Contrib Embryol* **1948**, 32, 133-203.
7. De Vries, P.A.; Saunders, J.A.de G.M. Development of the ventricles and spiral outflow tract of the human heart. *Contr Embryol Carnegie Inst,* **1962**, 37, 87-114.
8. Hochstetter F. Entwicklung des Blutgefässsystems. In *Handbuch der vergleichenden und experimentellen Entwicklungslehre der Wirbeltiere*, Hertwig, O., Ed.; Gustav Fischer: Jena, Germany, 1906; Volume 3, pp. 21–166.

982   9.   Tandler J. The development of the heart. In *Manual of Human Embryology*, Keibel, F.; Mall, F.P., Eds.;
983   Lippincott Company: Philadelphia & London, USA, Great Britain, 1912; Volume 2, pp. 534–570.

984   10. Kölliker, A. Die embryonalen Keimblätter und die Gewebe. Z wiss Zool 1884, 15, 179-213.

985   11. von Szily A. Über das Entstehen eines fibrillären Stützgewebes im Embryo und dessen Verhältnis zur
986   Glaskörperfrage. *Anat Hefte* **1908**, 35, 649-757.

987   12. Herxheimer G. Mißbildungen des Herzens und der großen Gefäße. In *Die Morphologie der Mißbildungen des*
988   *Menschen und der Tiere*, Schwalbe, O., Ed.; Gustav Fischer: Jena, Germany, 1910; Volume 3-3, pp. 339–504.

989   13. Davis, C.L. The cardiac jelly of the chick embryo (Abstract). *Anat Rec* **1924**, 27, 201.

990   14. FIPAT. Terminologia Embryologica. International Embryological Terminology. Georg Thieme Verlag:
991   Stuttgart, Germany, 2013

992   15. Manasek, F.J. The extracellular matrix: a dynamic component of the developing embryo. *Curr Top Dev Biol*
993   **1975**, 10, 35-120.

994   16. Barry, A. The functional significance of the cardiac jelly in the tubular heart of the chick embryo. *Anat Rec*
995   **1948**, 102, 289-298.

996   17. Camenisch, T.D.; Biesterfeldt, J.; Brehm-Gibson, T.; Bradley, J.; McDonald, J.A. Regulation of cardiac
997   cushion development by hyaluronan. *Exp Clin Cardiol* **2001**, 6, 4-10.

998   18. Manasek F. The extracellular matrix of the early embryonic heart. In *Perspectives in Cardiovascular Research*,
999   Lieberman, M.; Sano, T., Eds.; Raven Press: New York, USA, 1975; Volume 1, pp. 1–20.

1000 19. Nakamura, A.; Manasek, F.J. An experimental study of the shape and structure of isolated cardiac jelly. *J*
1001   *Embryol Exp Morphol* **1978**, 43, 167-183.

1002 20. Nakamura, A.; Manasek, F.J. An experimental study of the relation of cardiac jelly to the shape of the early
1003   chick embryonic heart. *J Embryol Exp Morphol* **1981**, 65, 235-256.

1004 21. Chapman, G. The hydrostatic skeleton in the invertebrates. *Biol Rev* **1958**, 33, 338-371.

1005 22. Chapman, G. Versatility of hydraulic systems. *J Exp Zool* **1975**, 194, 249-270.

1006 23. Kier, W.M. 2012. The diversity of hydrostatic skeletons. *J Exp Biol* **2012**, 215, 1247-1257.

1007 24. Manasek F.J.; Kulikowski, R.R.; Nakamura, A.; Nguyenphuc, Q.; Lacktis, J.W. Early heart development: a
1008   new model of cardiac morphogenesis. In *Growth of the Heart in Health and Disease*, Zak, R., Ed.; Raven Press:
1009   New York, USA, 1984, pp. 105–130.

1010 25. Baldwin, H.S.; Solursh, M. Degradation of hyaluronic acid does not prevent looping of the mammalian
1011   heart in situ. *Dev Biol* **1990**, 136, 555-559.

1012 26. Linask, K.K.; Han, M.D.; Linask, K.L.; Schlange, T.; Brand, T. Effect of antisense misexpression of CFC on
1013   downstream flectin protein expression during heart looping. *Dev Dyn* **2003**, 228, 217-230.

1014 27. Patten, B.M.; Kramer, T.; Barry, A. Valvular action in the embryonic chick heart by localized apposition of
1015   endocardial masses. *Anat Rec* **1948**, 102, 299-310.

1016 28. Little, C.D.; Rongish, B.J. Extracellular matrix during heart development. *Experentia* **1995**, 51, 873-882.

1017 29. Bowers, S.L.K.; Banerjee, I.; Baudino, T.A. The extracellular matrix: at the center of all. *J Mol Cell Cardiol*
1018   **2010**, 48, 474-482.

1019 30. Lockhart, M.; Wirrig, E.; Phelps, A.; Wessels, A. Extracellular matrix and heart development. *Birth Defects*
1020   *Res A* **2011**, 91, 535-550.

1021 31. Williams, C.; Black, L.D. The role of extracellular matrix in cardiac development. In *Biomaterials for cardiac*
1022   *regeneration*, Suuronen, E.J.; Ruel, M., Eds., Springer, **2015**, pp. 1-35.

1023 32. Kirby, M. Cardiac Development. Oxford University Press: New York, USA, 2007.

1024 33. Rosenthal, N.; Harvey, R.P. Heart Development and Regeneration. Vol 1. Academic Press: London, UK,
1025   2010.

1026 34. Granados-Riveron, J.T.; Brook, J.D. The impact of mechanical forces in heart development. *Circ Cardiovasc*
1027   *Genet* **2012**, 5, 132-142.

1028 35. Courchaine, K.; Rykiel, G.; Rugonyi, S. Influence of blood flow on cardiac development. *Prog Biophys Molec*
1029   *Biol* **2018**, 137, 95-110.

1030 36. Manasek, F.J. Embryonic development of the heart. I. A light and electron microscopic study of
1031   myocardial development in the early chick embryo. *J Morphol* **1968**, 125, 329-366.

1032 37. DeRuiter, M.C.; Poelmann, R.E.; VanderPlas-de Vries, I.; Mentink, M.M.T.; Gittenberger-de Groot, A.C.
1033   The development of the myocardium and endocardium in mouse embryos. Fusion of two heart tubes?
1034   *Anat Embryol* **1992**, 185, 461-473.

38. Sakai, T.; Hirota, A.; Kamino, K. Video-imaging assessment of initial beating patterns of the early embryonic chick heart. *Japan J Physiol* **1996**, 46, 465-472.

39. Sissman, J. Developmental landmarks in cardiac morphogenesis: comparative chronology. *Am J Cardiol* **1970**, 25, 141-148.

40. Kuhn, H.J.; Liebherr, G. The early development of the heart of *Tupaia belangeri*, with reference to other mammals. *Anat Embryol* **1987**, 176, 53-63.

41. Moorman, A.F.M.; Christoffels, V.M.; Anderson, R.H.; van den Hoff, M.J.B. The heart-forming fields: one or multiple. *Phil Trans. R Soc B* **2007**, 362, 1257-1265.

42. Bremer, J.L. The development of the aorta and aortic arches in rabbits. *Anat Rec* **1912**, 13, 111-128.

43. Dwinnell, L.A. Physiological contraction of the double hearts in rabbit embryos. *Exp Biol Med* **1939**, 42, 264-267.

44. Goss, C.M. The physiology of the embryonic mammalian heart before circulation. *Am J Physiol* **1942**, 137, 146-151.

45. Goss, C.M. Development of the median coordinated ventricle from the lateral hearts in rat embryos with three to six somites. *Anat Rec* **1952**, 112, 761-796.

46. Schulte, H.W. The fusion of the cardiac anlages and the formation of the cardiac loop in the domestic cat (Felis domestica). *Anat Rec* **1916**, 20, 45-72.

47. Steding,G.; Seidl, W.; Kluth, D.; Schulze, M. Die Entstehung des Endocard. Untersuchungen an Hühnerembryonen. *Verh Anat Ges* **1980**, 74, 365-367.

48. Hiruma, T.; Hirakow, R. An ultrastructural topographical study on myofibrillogenesis in the heart of the chick embryo during pulsation onset period. *Anat Embryol* **1985**, 172, 325-329.

49. Mohun, T.J.; Leong L.M.; Weninger, W.J.; Sparrow, D.B. The morphology of heart development in Xenopus laevis. *Dev Biol* **2000**, 218, 74-88.

50. Hempel, A.; Kühl, M. A matter of the heart: the African clawed frog *Xenopus* as a model for studying vertebrate cardiogenesis and congenital heart defects. *JCDD* **2016**, 3, 21. doi:10.3390/jcdd3020021

51. His, W. Anatomie menschlicher Embryonen III. Zur Geschichte der Organe. F.C.W. Vogel: Leipzig, Germany, 1885.

52. Mall, F.P. The development of the human heart. *Am J Anat* **1912**, 13, 49-298.

53. Manasek, F.J. 1970. Histogenesis of the embryonic myocardium. *Am J Cardiol* **1970**, 25, 149-168.

54. Icardo, J.M.; Fernandez-Terán, A. Morphologic study of ventricular trabeculation in the embryonic chick heart. *Acta Anat* (Basel) **1987**, 130, 264-274.

55. Männer, J.; Thrane, L.; Norozi, K.; Yelbuz, T.M. In vivo imaging of the cyclic changes in cross-sectional shape of the ventricular segment of pulsating embryonic chick hearts at stages 14 to 17: A contribution to the understanding of the ontogenesis of cardiac pumping function. *Dev Dyn* **2009**, 238, 3273-3284.

56. Christoffels, V.M.; Habets, P.E.; Franco, D.; de Jong, F.; Lamers, W.H.; Bao, Z.Z.; Palmers, S.; Biben, C.; Harvey, R.P.; Moorman, A.F.M. Chamber formation and morphogenesis of the mammalian heart. *Dev Biol* **2000**, 223, 266-278.

57. Markwald, R.R.; Fitzharris, T.P.; Manasek, F.J. Structural development of the endocardial cushions. *Am J Anat* **1977**, 148, 85-119.

58. Butcher, J.T.; McQuinn, T.C.; Sedmera, D.; Turner, C.; Markwald, R.R. Transitions in early embryonic atrioventricular valvular function correspond with changes in cushion biomechanics that are predicted by tissue composition. *Circ Res* **2007**, 100, 1503-1511.

59. Loumes, L.; Avrahami, I.; Gharib, M. Resonant pumping in a multilayer impedance pump. *Physics Fluids* **2008**, 20, 023103-1 - 023103-11.

60. Vogel, S. Pumps and pipes. Chapter 2 In *Vital circuits: on pumps, pipes, and the wondrous workings of circulatory systems*, Vogel, S., Ed.; Oxford University Press: New York, USA, 1992, pp. 19-42.

61. Schäfer, W. Some biomechanical aspects of continence function. *Scand J Urol Nephrol* (Suppl.) **2001**, 207, 44-60.

62. Wirtinger, W. Die Analyse der Wachstumsbewegungen und der Septierung des Herzschlauches. *Anat Anz* **1937**, 84, 33–97.

63. Butler, J.K. An experimental analysis of cardiac loop formation in the chick. MA Thesis, University of Texas, Austin, Texas USA, 1952.

64. Gittenberger-de Groot, A.C.; Bartelings, M.M.; Poelmann, R.E. Overview: Cardiac morphogenesis. In *Developmental Mechanisms of Heart Disease*, Clark, E.B.; Markwald, R.R.; Takao, A., Eds.; Futura: New York, USA, 1995, pp 157-168.

65. Männer, J. Ontogenetic development of the helical heart: Concepts and facts. *Eur J Cardio Thorac Surg* **2006**, 295, S69-S74.

66. Männer, J.; Thrane, L.; Norozi, K.; Yelbuz, T.M. High resolution in vivo imaging of the cross-sectional deformations of contracting embryonic heart loops using optical coherence tomography. *Dev Dyn* **2008**, 237, 953-961.

67. Garita, B.; Jenkins, M.W.; Han, M.; Zhou, C.; Van Auker, M.; Rollins, A.M.; Watanabe, M.; Fujimoto, J.G.; Linask, K.K. Blood flow dynamics of one cardiac cycle and relationship to mechanotransduction and trabeculation during heart looping. *Am J Physiol Heart Circ Physiol* **2011** 300, H879-H891.

68. Happel, C.M.; Thommes, J.; Thrane, L.; Männer, J.; Ortmaier, T.; Heimann, B.; Yelbuz, T.M. Rotationally acquired four-dimensional optical coherence tomography of embryonic chick hearts using retrospective gating on the common central A-scan. *J Biomed Optics* **2011**, 16, 096007-1 – 09667-6.

69. Taber, L.A.; Perucchio, R. Modeling heart development. *J Elasticity* **2000**, 61:165-197.

70. Sarin, V.B.; Mehrotra, R. Stenotic effects in a tube of elliptic cross-section at low Reynolds numbers. *Int J Biomed Comput* **1992**, 30:137-146.

71. Hu, N.; Connuck D.M.; Keller, B.B.; Clark, E.B. Diastolic filling characteristics in the stage 12 to 27 chick embryo ventricle. *Pediatr Res* **1991**, 29:334-337.

72. Nakamura, A.; Manasek, F.J. Cardiac jelly fibrils: their distribution and organization. In *Morphogenesis and malformation of the cardiovascular system*, Birth Defects Orig Article Ser Volume 14, Rosenquist, G.; Bergsma, D., Eds.; Liss: New York, USA, 1978, pp. 229-250.

73. Nakamura, A.; Kulikowski, R.R.; Lacktis, J.W.; Manasek, F.J. Heart looping: a regulated response to deforming forces. In *Etiology and morphogenesis of congenital heart disease*, Van Praagh, R.; Takao, A., Eds.; Futura: New York, USA, 1980, pp. 81-98.

74. Hurle, J.M.; Icardo, J.M.; Ojeda, J.L. Compositional and structural heterogenicity of the cardiac jelly of the chick embryo tubular heart: a TEM, SEM and histochemical study. *J Embryol Morph* **1980**, 56, 211-223.

75. Kielty, C.M. Fell-Muir lecture: fibrillin microfibrils: structural tensometers of elastic tissues? *Int J Exp Path* **2017**, 98, 172-190.

76. Gambini, C.; Abou, B.; Ponton, A.; Cornelissen, A.J.M. Micro- and macrorheology of jellyfish extracellular matrix. *Biophys J* **2012**, 102, 1-9.

77. Weber, C.; Schmid, V. The fibrous system in the extracellular matrix of hydromedusae. *Tiss Cell* **1985**, 17, 811-822.

78. Megill, W.M.; Gosline, J.M.; Blake, R.W. The modulus of elasticity of fibrillin-containing fibres in the mesoglea of the hydromedusa Polyorchis penicillatus. *J Exp Biol* **2005**, 208, 3819-3834.

79. Reber-Müller, S.; Spissinger, T.; Schuchert, P.; Spring, J.; Schmid, V. An extracellular matrix protein of jellyfish homologous to mammalian fibrillins forms different fibrils depending on the life stage of the animal. *Dev Biol* **1995**, 169, 662-672.

80. Gladfelter, W.B. Structure and function of the locomotory system of Polyorchis montereyensis (Cnidari, Hydrozoa). *Helgoland Wiss Meer* **1972**, 23, 38-79.

81. Baldwin, H.S.; Lloyd, T.R.; Solursh, M. Hyaluronate degradation affects ventricular function of the early postlooped embryonic rat heart in situ. Circ Res **1994**, 74, 244-252.

82. Hierck, B.P.; Van der Heiden, K.; Poelma, C.; Westerweel, J.; Poelmann, R.E. Fluid shear stress and inner curvature remodeling of the embryonic heart. Choosing the right lane! *TSW Dev & Embryol* **2008**, 8, 212-222.

83. Ben-Shachar, G.; Arcilla, R.A.; Lucas, R.V.; Manasek, F.J. Ventricular trabeculations in the chick embryo heart and their contribution to ventricular and muscular septal development. *Circ Res* **1985**, 57, 759-766.

84. Reichel, T. Cardiac looping und die frühe Topogenese der AV-Region: Untersuchungen an Hühnerembryonen. Doctoral Thesis, UMG, University of Göttingen, Göttingen, Germany, 2016.

85. De la Cruz, M.V.; Sanchez-Gomez, C. Straight tube heart. Primitive cardiac cavities vs. primitive cardiac segments. In *Living Morphogenesis of the Heart*, De la Cruz, M.V.; Markwald, R.R., Eds.; Birkhäuser: Boston, USA, 1999, pp. 85–98.

86. Hu, N.; Clark, E.B. Hemodynamics of the stage 12 to 29 chick embryo. *Circ Res* **1989**, 65, 1665-1670.

87. Steinhoff, W. Zur Entwicklung der terminalen Strombahn im Hühnerherzen. *Anat Embryol* **1971**, 134, 255-277.

88. Goor, D.A.; Lillehei, C.W. The embryology of the heart. Chapter 2 In *Congenital Malformations of the Heart. Embryology, Anatomy, and Operative Considerations*, Goor, D.A.; Lillehei, C.W., Eds.; Grune & Stratton: New York, USA, 1975, pp. 38-102.

89. Bennett, H.S. The development of the blood supply to the heart of the pig embryo. *Am J Anat* **1936**, 60, 27-53.

90. Virágh, S.; Challice, C.E. The origin of the epicardium and the embryonic myocardial circulation in the mouse. *Anat Rec* **1981**, 201, 157-168.

91. Sedmera, D.; Pexieder, T.; Hu, N.; Clark, E.B. Developmental changes in the myocardial architecture of the chick. *Anat Rec* **1997**, 248, 421-432.

92. Chuck, E.T.; Meyers, K.; France, D.; Creazzo, T.L.; Morley, G.E. Transitions in ventricular activation revealed by two-dimensional optical mapping. *Anat Rec A* **2004**, 280A, 990-1000.

93. Sedmera, D.; Reckova, M.; Bigelow, M.R.; DeAlmeida, A.; Stanley, C.P.; Mikawa, T.; Gourdie, R.G.; Thompson, R.P. Developmental transitions in electric activation patterns in chick embryonic heart. *Anat Rec A* **2004**, 280A, 1001-1009.

94. Moorman, A.F.; Christoffels, V.M. Cardiac chamber formation: development, genes, and evolution. *Physiol Rev* **2003**, 83, 1223-1267.

95. Sedmera, D.; McQuinn, T. Embryogenesis of the heart muscle. *Heart Failure Clin* **2008**, 4, 235-245.

96. D'Amato, G.; Luxán, G.; de la Pompa, J.L. Notch signaling in ventricular chamber development and cardiomyopathy. *FEBS J* **2016**, 283, 4223-4237.

97. Gitler, A.D.; Lu, M.M.; Jiang, Y.Q.; Epstein, J.A.; Gruber, P.J. Molecular markers of endocardial cushion development. *Dev Dyn* **2003**, 228, 643-650.

98. Person, A.D.; Klever, S.E.; Runyan, R.B. Cell biology of cardiac cushion development. *Int Rev Cytol* **2005**, 243, 287-335.

99. Butcher, J.T.; Markwald, R.R. Valvulogenesis: the moving target. *Philos Trans R Soc Lond B Biol Sci* **2007**, 362, 1489-1503.

100. Bremer, J.L. An interpretation of the development of the heart. Part II. The left aorta of reptiles. *Am J Anat* **1928**, 42, 307-369.

101. Ramsdell, A.F. Left-right asymmetry and congenital cardiac defects: getting to the heart of the matter in vertebrate left-right axis determination. *Dev Biol* **2005**, 288, 1-20.

102. Dominguez, J.N.; Meilhac, S.M.; Bland, Y.S.; Buckingham, M.E.; Brown, N.A. Asymmetric fate of the posterior part of the second heart field results in unexpected left/right contributions to both poles of the heart. *Circ Res* **2012**, 111, 1323-1335.

103. Wu, B.; Wang, Y.; Xiao, F.; Butcher, J.T. Developmental mechanisms of aortic valve malformation and disease. *Annu Rev Physiol* **2017**, 79, 21-41.

104. Sangvichien, S. Induction of reversal of the heart beat in chick embryos. *Anat Rec* **1952**, 112, 529-538.

105. Benninghoff, A. Über die Beziehungen des Reizleitungssystems und der Papillarmuskeln zu den Konturfasern des Herzschlauches. *Anat Anz* **1923**, 57, 185-208.

106. Boucek, R.J.; Murphy, W.P.; Paff, G.H. Electrical and mechanical properties of chick embryo heart chambers. *Circ Res* **1959**, 7, 787-793.

107. De Jong, F.; Opthof, T.; Wilde, A.A.; Janse, M.J.; Charles, R.; Lamers, W.H.; Moorman, A.F. Persisting zones of slow impulse conduction in developing chicken hearts. *Circ Res* **1992**, 71, 240-250.

108. Sedmera, D.; Pexieder, T.; Vuillemin, M.; Thompson, R.P.; Anderson, R.H. Developmental patterning of the myocardium. *Anat Rec* **2000**, 258, 319-337.

109. Camenisch, T.D.; Spicer, A.P.; Brehm-Gibson, T.; Biesterfeldt, J.; Augustine, M.L.; Calabro, A. Jr; Kubalak, S.; Klewer, S.E.; McDonald, J.A. Disruption of hyaluronan synthase-2 abrogates normal cardiac morphogenesis and hyaluronan-mediated transformation of epithelium to mesenchyme. *J Clin Invest* **2000**, 106, 349-360.

110. Greil, A. Beiträge zur vergleichenden Anatomie und Entwicklungsgeschichte des Herzens und des Truncus arteriosus der Wirbeltiere. *Morphol Jahrbuch* **1903**, 31, 123-310.

111. Galdos, F.X.; Guo, Y.; Paige, S.L.; VanDusen, N.J.; Wu, S.M.; Wu, W.T. Cardiac chamber regeneration. Lessons from development. *Circ Res* **2017**, 120, 941-959.

1193   112. Samsa, L.A.; Yang, B.; Liu, J. Embryonic cardiac chamber maturation: trabeculation, conduction and
1194   cardiomyocyte proliferation. *Am J Med Genet C Semin Med Genet* **2013**, 163, 157-168.
1195   113. Wu, M. Mechanisms of trabecular formation and specification during cardiogenesis. *Pediatr Cardiol* **2018**,
1196   39, 1082-1089.
1197   114. Soufan, A.; van den Berg, G.; Ruijter, J.M.; de Boer, P.A.J.; van den Hoff, M.J.B.; Moorman, A.F.M.
1198   Regionalized sequence of myocardial cell growth and proliferation characterizes early chamber formation.
1199   *Circ Res* **2006**, 99, 545-552.
1200   115. Sizarov, A.; Ya, J.; de Boer, B.A.; Lamers, W.H.; Christoffels, V.M.; Moorman, A.F.M. Formation of the
1201   building plan of the human heart. Morphogenesis, growth, and differentiation. *Circulation* **2011**, 123,
1202   1125-1135.